Guide-independent DNA cleavage by archaeal Argonaute from *Methanocaldococcus jannaschii*

Adrian Zander[1,#], Sarah Willkomm[1,#], Sapir Ofer[2], Marleen van Wolferen[3], Luisa Egert[1], Sabine Buchmeier[4], Sarah Stöckl[1], Philip Tinnefeld[4], Sabine Schneider[5], Andreas Klingl[6], Sonja-Verena Albers[3], Finn Werner[2], Dina Grohmann[1,*]

[1]Department of Microbiology & Archaea Centre, University of Regensburg, Regensburg, 93053, Germany

[2]Institute for Structural and Molecular Biology, Division of Biosciences, University College London, London WC1E 6BT, United Kingdom

[3] Molecular Biology of Archaea, Institute of Biology II, University of Freiburg, Microbiology, Schaenzlestraße 1, 79104 Freiburg, Germany

[4]Institute of Physical and Theoretical Chemistry – NanoBioSciences, Technische Universität Braunschweig-BRICS, Rebenring 56, 38106 Braunschweig, Germany

[5]Center for Integrated Protein Science Munich CIPSM, Department of Chemistry, Technische Universität München, Lichtenbergstrasse 4, 85748 Garching, Germany

[6]Biocentre of the LMU Munich, Department Biology I – Plant Development, Großhadernerstr. 2-4, 82152 Planegg-Martinstried, Germany

[#]These authors contributed equally

*For correspondence: dina.grohmann@ur.de (DG)

Keywords: Argonaute, archaea, DNA-guided gene silencing

Abstract

Prokaryotic Argonaute proteins acquire guide strands derived from invading or mobile genetic elements via an unknown pathway to direct guide-dependent cleavage of foreign DNA. Here, we report that Argonaute from the archaeal organism *Methanocaldococcus jannaschii* (MjAgo) possesses two modes of action: the canonical guide-dependent endonuclease activity and a non-guided DNA endonuclease activity. The latter allows MjAgo to process long double stranded DNAs, including circular plasmid DNAs and genomic DNAs. Degradation of substrates in a guide-independent fashion primes MjAgo for subsequent rounds of DNA cleavage. Chromatinised genomic DNA is resistant to MjAgo degradation and recombinant histones protect DNA from cleavage *in vitro*. Mutational analysis shows that key residues important for guide-dependent target processing are also involved in guide-independent MjAgo function. This is the first-time characterisation of a guide-independent cleavage activity for an Argonaute protein potentially serving as guide biogenesis pathway in a prokaryotic system.

Introduction

Argonaute (Ago) proteins are crucially involved in RNA-guided or DNA-guided degradation of target nucleic acids.[1-3] Present in all three domains of life, they bind guide strands *in vivo* to target complementary nucleic acids. Eukaryotic Agos interact with cytoplasmic RNA substrates 18–23 bp in length [4-6] while prokaryotic Agos (pAgos) bind and process a variety of DNA and RNA substrates.[7-11] Among them, Agos from the archaeal organisms *Methanocaldococcus jannaschii* (MjAgo), *Pyrococcus furiosus* (PfAgo) and *Natronobacterium gregoryi* (NgAgo) are the only Ago variants that exclusively cleave DNA substrates using a DNA guide *in vitro.*[7,11-13] Guide recognition is mediated by a phosphate group at the guide's 5'-end, which is coordinated in the Mid domain by conserved amino-acid side chain interactions.[14-18] One exception are the recently characterized bacterial Agos from *Marinitoga piezophila* (MpAgo) and *Thermotoga profunda* (TpAgo), which recognise RNA guides with a 5'-hydroxyl group.[19] Loaded with the guide, Ago binds partially or fully complementary target nucleic acids via Watson-Crick base pairing. Only fully complementary target strands are cleaved by Ago. The catalytic site resides in the PIWI domain. Notably, numerous pAgos, especially short Argonaute variants, have an incomplete catalytic site rendering them inactive.[2]

While the structural organization of pAgos is well understood, their biological role is still not fully revealed. *In vivo* studies have only been reported for the bacterial organisms *Thermus thermophilus* (Tt) and *Rhodobacter sphaeroides* (Rs). In both cases, Ago appears to play a role in host defence.[8,20] TtAgo acquires guide DNAs 13-25 nt in length that carry the canonical 5'-phosphate. Overexpression of TtAgo in *T.thermophilus* leads to its association with DNA sequences mainly derived from the TtAgo expression plasmid.[8] TtAgo, MpAgo and NgAgo cleave plasmids complementary to their guide DNA by nicking both strands of the plasmid DNA.[8,19,21] In contrast, RsAgo is most probably involved in RNA-guided DNA silencing.[20] The majority of sequences acquired by RsAgo map to genome-encoded foreign nucleic acids like transposons and phage genes.[20] It was suggested that the catalytically inactive RsAgo acts in concert with a nuclease, which is encoded in the same operon, thereby mediating RNA-guided silencing in *R. sphaeroides*.

In this study, we describe the guide-independent endonuclease activity of the archaeal MjAgo. We show that MjAgo can process long dsDNAs including plasmids and genomic DNA in a guide-independent manner, which leads to the generation of cleavage products potentially suitable as guides. Using these cleavage products in a second cleavage round accelerates processing of the original substrate DNA suggesting a priming mechanism. Only the chromatinised state of *M.jannaschii's* genomic DNA is protected against MjAgo-mediated degradation, and histone proteins are likely to confer this protection. Additionally, our structure-based mutational analysis reveals amino acids and structural elements of crucial importance for the guide-independent cleavage activity of MjAgo. Taken together, our findings support a scenario in which the non-guided endonuclease activity of MjAgo represents a mechanism to protect a prokaryotic organism against foreign genetic elements.

RESULTS

MjAgo can utilize non-canonical DNA guides for cleavage of DNA targets

First, we analysed the guide length tolerance of MjAgo. We tested 5'-phosphorylated DNA guides 13–23 nt in length in a guide-dependent target cleavage assay (**Figure 1a**). Starting from a minimal guide length of 15 nt, MjAgo accepted all guide lengths up to 23 nt (**Figure 1b**). We also found efficient cleavage of a non-canonical substrate (41 nt guide / 41 nt target) even without a 5'-phosphate (**Figure 1c,d and Supplementary Figure 1**). None of the substrates was cleaved by the catalytic mutant MjAgo^{E541A} (**Supplementary Figure 2**). Next, we tested whether MjAgo exhibits orientated loading and cleavage of the 41 nt guide/41 nt target substrate using target strands that either carry the fluorescent label at the 5'-end or towards the 3'-end together with guide strands with and without a 5'-phosphate group (**Figure 1e**). In case of a 5'-phosphorylated 41nt guide, the production of a canonical cleavage product was observed with cleavage occurring opposite nucleotide 10/11 of the guide strand. However, the majority of the substrate is preferentially cleaved from the 5'-end of the target strand in a stepwise manner (**Figure 1f**). From a structural perspective, it is not feasible that both ends of a 41 nt long guide are accommodated in the Mid and PAZ domain indicating that MjAgo employs a non-canonical binding and cleavage mechanism.

MjAgo cleaves long linear and circular double-stranded DNA in a guide-independent fashion

Next, we tested significantly longer substrates and incubated MjAgo with a 750 bp dsDNA and circular double-stranded plasmid DNAs. In both cases, we found cleavage of the substrate in a guide-independent manner (the MjAgo^{E541A} mutant did not process these DNAs) (**Figure 2a,c,d)**. The DNA is gradually cleaved over time (**Supplementary Figure 3**) until final cleavage products smaller than 100 bp accumulate (**Figure 2 and 3**). EDTA prevents cleavage of long dsDNA by MjAgo (**Supplementary Figure 4**) suggesting that the conserved catalytic tetrad, which coordinates two metal ions, carries out the cleavage reaction. DNA degradation occurs quickly at physiological relevant high temperatures of 75°C-85°C **(Figure 2d)**.

To visualise MjAgo associated with long dsDNA fragments (**Figure 2B**) we used transmission electron microscopy (TEM). In the transmission electron micrographs, the MjAgo protein alone, naked linear dsDNA (750 bp) as well as interactions of MjAgo with DNA were observed.

Furthermore, we detected low levels of MjAgo protein in *M.jannaschii* whole cell lysates using anti MjAgo antibodies (**Supplementary Figure 5**) indicating a constitutive expression of MjAgo under normal growth conditions without the requirement of external factors, e.g. infection by a virus or invasion of foreign genetic material. Thus, we tested whether the genomic DNA (gDNA) of *M. jannaschii* is protected against MjAgo-mediated degradation. MjAgo cleaves highly purified "naked" gDNA while chromatinised DNA is resistant to degradation (**Figure 2e**). In order to investigate whether the abundant A3 histone from *M. jannaschii* is the agent that confers Ago resistance, we reconstituted recombinant histone A3 from *M. jannaschii* with a short dsDNA (750 bp) template to enable histone-DNA complex formation. The latter were not significantly degraded by MjAgo (**Figure 2f**) indicating that histone-bound DNA is not accessible for MjAgo. Interestingly, when low amounts of A3 are added, DNA becomes accessible for MjAgo leading to a ladder-like degradation pattern reminiscent of patterns created by digestion of chromatin with Micrococcal nuclease (MNase) (**Supplementary Figure 6**).

Different methylation patterns were described for gDNAs from archaeal species.[22] Therefore, we tested whether methylation signatures serve as recognition sites for MjAgo cleavage as some nucleases show reduced or no activity on methylated substrates. [23] Genomic DNAs from *M. jannaschii* and *P. furiosus* carry a m4C, m6A, m5C methylation, whereas gDNA from *S. acidocaldarius* is only methylated at position 4C and 5C. Genomic DNAs from *P. furiosus* and *S. acidocaldarius* were degraded by MjAgo (**Supplementary Figure 7a**). Additionally, we used bacterial-purified plasmids that carried either the dam or the dcm methylation or both. All plasmids were degraded by MjAgo (**Supplementary Figure 7b**). These data indicate that the bacterial and archaeal methylation patterns do not influence MjAgo activity.

In order to determine the size of the final degradation products produced by MjAgo, we radiolabelled the cleavage products (**Figure 3a**) at the 5'-end with or without prior removal of a 5'-terminal phosphate group and analysed the length distribution

(**Figure 3b**). Nucleolytic degradation of dsDNA by MjAgo yielded mainly final products in the range of 8-13 nt with weak bands visible for longer products (14 to approximately 17 nt). Radiolabelling was also successful when samples without 5'-phosphate removal were used suggesting that MjAgo creates fragments with or without a 5'-terminal phosphate group. Cleavage assays showed that unphosphorylated guides can direct MjAgo-mediated target cleavage (**Supplementary Figure 8**).

We tested whether these final degradation products can serve as guides for sequence-specific degradation in a subsequent round of plasmid cleavage. Plasmid DNA degradation is significantly accelerated if the reaction is supplemented with the final products of a previous cleavage reaction using the same plasmid (**Figure 3c**) indicating this might be one component of a priming mechanism. However, in case a plasmid unrelated in sequence is used, the cleavage reaction also appears to be faster as compared to a reaction without pre-digestion of a prior plasmid but is still significantly slower as compared to the reaction with pre-digestion of the same plasmid. This unspecific acceleration might be another component of a priming mechanism. Possibly, one round of MjAgo-mediated cleavage during the pre-digestion of a plasmid induces a cleavage-competent conformational state that leads to a fast processing of substrates in general.

Next, we analysed whether 21 nt 5'-phosphorylated guides direct specific nicking and linearization of a plasmid as it has been demonstrated for other prokaryotic Agos. [8,19,21] However, no specific band indicative for nicking or linearization of the plasmid was observed (**Figure 3d**).

Mutational analysis of MjAgo-mediated non-canonical DNA substrate cleavage

In order to identify the structural elements that are important for the guide-independent activity of MjAgo, we carried out a mutational analysis. MjAgo anchors the 5'- and 3'-end of a canonical guide strand in dedicated binding pockets in the Mid and PAZ domain, respectively (PDB: 5G5S and 5G5T).[1,24] We tested whether mutations in the functional domains of MjAgo (**Figure 4a**) affect the plasmid cleavage activity. PAZ binding pocket mutants (Y194A, H213A, Y217A, E246A) showed significantly reduced cleavage activity (**Figure 4b**) suggesting that the

interaction between DNA and the PAZ domain is important for the guide-independent cleavage activity. The PAZ domain undergoes a conformational transition upon loading of the guide DNA (**Supplementary Figure 9**).[24] In the apo enzyme, residues N170 (PAZ domain) and D438 (Mid domain) are in close proximity potentially stabilising the closed conformation of apo MjAgo (**Figure 4a**, inset). We mutated position N170 and found that the mutant was active suggesting that an interruption of the putative N170-D438 interaction does not influence MjAgo's guide-independent cleavage activity. Additionally, we tested MjAgo variants with mutations in helix 8 (L270P and W274V). Helix 8 corresponds to helix 7 in hAgo2, a mobile element important for efficient formation of the guide/target duplex. [15,18,24,25] Helix 8 mutations were active albeit with slightly reduced cleavage activity. Mutations of amino acids lining a putative secondary nucleic acid binding channel (F572A, Q574A, N575A), a feature we recently identified in the crystal structures of MjAgo (PDB: 5G5T)[24] (**Supplementary Figure 10**), did not significantly reduce cleavage activity. Only the mutant F572A showed a slightly reduced activity, which might be due to the close proximity of this residue to the active site. Mutations of amino acids that are directly involved in the coordination of the 5'-end of a conventional guide (K435A, D438P, Q457A, N458A, Q479A, K483A) lead only in case of D438P and K483A to complete inactivation or strongly reduced activity.

Among these mutants, only mutation of residues Y194, E246 and K483 seem to be critical for both modes of MjAgo activity. K483 is involved in the coordination of a magnesium ion in the Mid binding pocket and is of crucial importance for MjAgo activity. Interestingly, residues Q457, N458, L270, F572, Q574 and N575 are only important for the guide-dependent cleavage activity, as all of these mutants are catalytically inactive using a canonical substrate. [24]

MjAgo associates with small DNA *in vivo* and impairs growth in a heterologous archaeal expression system

Having established that MjAgo is able to process genomic DNA from foreign species *in vitro*, we next tested whether cleavage of DNA occurs also *in vivo* and affects the viability of the organism used for heterologous expression of MjAgo. We

transformed suitable expression plasmids encoding either wildtype MjAgo or the catalytically inactive mutant into *S. acidocaldarius* and *E. coli*.

We expressed and purified recombinant MjAgo from *E. coli* lysate via affinity chromatography and subsequently isolated nucleic acids associated with MjAgo (nucleic acids remain bound to MjAgo if the extraction and purification is carried out at 4°C but not if carried out at room temperature). These nucleic acids are smaller than 100 bases and resistant to RNases but sensitive to DNase treatment (**Figure 3e**) suggesting that MjAgo interacts with short DNAs *in vivo* in *E.coli.* These DNAs might represent MjAgo degradation products. However, growth of *E.coli* was not impaired by overexpression of MjAgo, most likely because DNA replication is an extremely fast process in *E. coli* but the guide-independent cleavage activity of MjAgo is very slow at 37°C. In order to exclude the possibility that traces of these short nucleic acids remain bound to MjAgo during protein preparation at room temperature and serve as guides, we purified MjAgo-associated nucleic acids and added them back to a reaction containing MjAgo and plasmid DNA at defined concentrations (**Supplementary Figure 11**). In case these DNAs serve as unspecific guides for MjAgo, an acceleration of the cleavage reaction should be observed. However, the presence of these short DNAs (**Supplementary Figure 11a**) did neither influence nor stimulate MjAgo-mediated cleavage of plasmid DNA even at high concentrations (**Supplementary Figure 11b**). Consequently, MjAgo activity is genuinely a guide-independent activity.

Since no genetic system is established for *M. jannaschii*, we were not able to affinity-purify endogeneous MjAgo and to isolate nucleic acids associated with MjAgo *in vivo*. However, *S. acidocaldarius* is a genetically tractable archaeal organism that does not encode an Argonaute variant but – like *M. jannaschii* - is a thermophile with a comparable optimal growth temperature (70-80°C). Thus, using *S. acidocaldarius* as heterologous expression host, we were able to study MjAgo activity in an archaeal organism at near optimal temperatures. We found approximately 25-fold less transformants when using a plasmid encoding wildtype MjAgo as compared to the catalytically inactive mutant (wt MjAgo: 13 colonies vs $MjAgo^{E541A}$: 341 colonies) for transformation. MjAgo immunodetection in whole cell extracts verified MjAgo expression in *S. acidcocaldarius*. While we found good

expression levels of MjAgo in case of the catalytic mutant, almost no MjAgo was detectable in case of the transformants that expressed wildtype MjAgo (**Supplementary Figure 12a/b**). To find out whether the reduced protein level is due to proteolytic degradation of wt MjAgo or reduced plasmids levels in the cells, we PCR-amplified the expression plasmid and found reduced levels of the MjAgo wt expression plasmid as compared to the plasmid levels of the catalytic mutant in the cell lysate (**Supplementary Figure 12c**). These results suggest that MjAgo is active when expressed in the crenarchaeal organism *S. acidocaldarius,* which negatively affects the viability of the organism possibly due to MjAgo-mediated degradation of *Sulfolobus*' gDNA. In contrast to *M. jannaschii*, *Sulfolobus* does not encode histones but histone-like proteins (e.g. Alba, Cren7 and Sul7) that compact the genome for example via loop formation. However, the interaction of Alba is less stable than the tight wrapping of DNA in nucleosomes most likely leaving the gDNA more susceptible for MjAgo action. [26]

DISCUSSION

Some prokaryotic Agos use short guides to direct guide-dependent plasmid nicking or double-strand cleavage of plasmid DNA at a single site. Here, we show that the archaeal Ago from *M. jannaschii* works as both, a guided and guide-independent endonuclease, the latter enabling the processing of non-canonical substrates like linear and circular dsDNAs potentially driving the silencing of invading and self-replicating genetic elements.

Testing the substrate spectrum of MjAgo revealed that MjAgo requires a minimal guide length of 15 nt and highest cleavage efficiency was observed with a 19 nt guide in guide-dependent DNA cleavage reactions. This is in good agreement with other prokaryotic Agos that utilise guides in the size range of 14-25 nt.[7,8,12,19-21] Base pairing of a 14-15 nt guide with a target appears to be the minimally required length in all characterised pAgos yielding a stable duplex even at high reaction temperatures typical for thermophiles. The duplex stability must be enhanced beyond the thermal stability of the dsDNA by the intricate network of interactions in the Mid binding pocket and the seed region of the guide to ensure that the substrate remains hybridised during a single round of target cleavage. We additionally observed that MjAgo employs guides well above the canonical guide lengths (e.g. using a 41 nt guide), which has also been reported recently for MpAgo.[19] Structural studies showed that the 5'- and 3'-end of the guide is anchored in the Mid and PAZ binding pocket, respectively.[16,19,21] The 3'-end is released from the PAZ domain upon target loading.[10,11] In case of a 41 nt guide, sterical constraints would not allow the docking of the 5'- and the 3'-end in the binding pockets. We found that the 41 nt guide is nevertheless associated with the Mid domain pocket when a 5'-phosphate is present as the canonical cleavage product is observed. This reaction competes with a cleavage reaction that preferentially starts from the 3'-end of the guide and leads to a stepwise processing of the target. Cleavage generates a new phosphate group that could direct the subsequent cleavage reaction resulting in an apparent stepwise degradation of the labelled target. However, the 3'-end cleavage mode is slower than the phosphate-guided reaction suggesting that the substrate is not ideally positioned for efficient cleavage in the Mid domain binding pocket. Interestingly, hAgo2 is also capable to process non-canonical long dsRNAs. Cheloufi *et al* showed

that hAgo2 degrades the 41 nt long pre-miRNA-451 in a Dicer-independent manner.[27] hAgo2 cleaves this substrate at the canonical cleavage site suggesting that the 5'-end of the dsRNA is anchored in the Mid domain and hAgo2 is able to accommodate this species without an interaction of the 3'-end and the PAZ domain.

A gradual degradation is also observed when MjAgo processes long linear dsDNA, plasmid DNA or gDNA. EM images revealed that MjAgo associates with dsDNA and might employ a comparable sliding mechanism as described for hAgo2 to search for the terminus of the DNA. [28] In case of circular DNA, first, cleavage of both strands has to occur to result in the observed linearized form of the plasmid. This step appears to be more efficient at elevated temperatures. Here, thermal breathing of the DNA is enhanced resulting in transiently opened DNA that could serve as entry point for MjAgo. Nicking of one of the strands creates a free 5'-phosphate group, which can be positioned in the Mid binding pocket followed by cleavage of the second strand in close proximity that is detectable as linearized plasmid. Mutational analysis underscores the importance of the magnesium in the Mid binding pocket as mutation of K483 involved in the coordination of the magnesium and the terminal base leads to strongly reduced plasmid degradation activity. Equally important is D438, which is part of the so-called nucleotide-specificity loop – a conserved feature for the coordination of the 5'-end terminal nucleotide.[17] In MjAgo, D438 is part of a 3_{10} helix that forms upon formation of the binary guide-MjAgo complex.[24] Interruption of this helix reduces the guide-dependent and guide-independent MjAgo activity. Mutational analysis also revealed that the PAZ domain is critical for MjAgo-mediated plasmid degradation. Even though the long substrates cannot be anchored in both, the Mid and PAZ pocket, the PAZ domain has a general affinity for nucleic acids.[16] In fact, all pAgos that show guide-dependent plasmid DNA cleavage have to accommodate at least three nucleic acid strands. So far, no structural or mechanistic data are available that would answer the question how the substrate is accommodated when pAgos process plasmids. In MjAgo, a second positively charged nucleic acid binding channel is important for the efficient guide-dependent DNA endonuclease activity of MjAgo (**Supplementary Figure 10**).[24] This channel might provide space for one of the DNA strands handled by MjAgo during plasmid processing. It has been proposed that the channel formed in between the PAZ- and

N-terminal domain accommodates the target strand.[29] It would be conceivable that in MjAgo, strand separation is achieved by guiding one of the DNA strands through the primary (PAZ/N-terminal cleft) and secondary DNA binding channel (PIWI/N-terminal tunnel) with strand annealing after both strands have passed the N-terminal domain. However, mutational analysis of residues lining this putative secondary binding channel did not reveal a role of this channel in guide-independent cleavage. Recently, the structure of RsAgo in complex with a guide and target strand has been solved.[21] Here, base pairing of the guide/target duplex is maintained up to nucleotide 18 due to a slightly altered orientation of the N-terminal domain ('packing-type' N-terminal domain). In structures of substrate-associated TtAgo, the guide and target strands are separated after nucleotide 16 by the action of the N-terminal domain ('wedge-type' N-terminal domain).[10,30] These examples demonstrate that substrate positioning in pAgo variants does not follow a conserved pathway and MjAgo might bind nucleic acids in yet another slightly different configuration. A secondary DNA binding channel has not been identified in other pAgos yet rendering MjAgo the only characterised Ago variant that possesses additional structural features that might be involved in non-guided DNA endonuclease activity (**Supplementary Figure 13**).

Taken together, a picture of the *in vivo* function of MjAgo emerges (**Figure 5a**). MjAgo might serve as a safeguard system that, upon invasion of foreign nucleic acids like plasmids or viral DNA, is able to degrade these DNAs in a non-specific fashion via the guide-independent endonuclease function. The circular 1.7 Mb genome and the two extrachromosomal elements of *M. jannaschii* are inert against Ago, likely because histones intimately interact with the DNA and thus deny Ago access. In conjunction with the data collected from heterologous expression of MjAgo in *S. acidocaldarius*, an organism which does not encode any histones, these results lead to the hypothesis that the chromatinisation state of the DNA would serve a "self vs non-self" discrimination marker. This wave of defence is relatively slow but followed by a faster phase. Potentially, guides are recruited during the first step of guide-independent MjAgo action priming MjAgo for a second round of guide-dependent cleavage with significantly increased substrate turnover. In contrast to the CRISPR-Cas systems, the postulated MjAgo-mediated defence system does not possess a

memory. Earlier experiments showed that guide strands dissociate from MjAgo[11], which ultimately allows re-priming of the cellular MjAgo pool. Interestingly, PfAgo does not exhibit complete degradation but only linearization of plasmid DNA in a guide-independent manner[7]. The genomic context of the MjAgo gene (**Figure 5b**) also hints to the possibility that MjAgo is involved in DNA repair and/or recombination processes and its catalytic activity might be regulated by so far unknown proteins.

Even though guide sequences derived from exogenous plasmids, transposable elements and cellular transcripts were found to be associated with TtAgo and RsAgo *in vivo*, the biology of guide strand generation remained elusive as no pre-processing enzyme comparable to the eukaryotic Dicer nuclease could be identified so far that might fulfil this function. The non-canonical substrate usage of MjAgo provides a first mechanistic rational how Ago can be primed in prokaryotic organisms. However, in other prokaryotes different mechanisms seem to be in place. They remain to be identified, since to date no guide-independent endonucleolytic degradation of plasmid DNA was demonstrated for other guide-dependent DNA-silencing enzymes including TtAgo, NgAgo, MpAgo, PfAgo and RsAgo.

Methods

Protein preparation

Recombinant Argonaute from *M. jannaschii* was produced as described previously.[11] In brief, MjAgo was expressed in *E.coli* Rosetta(DE3)pLysS cells (Novagen). Cells were grown for 16h at 37°C after induction of expression with 1 mM IPTG. After harvesting the cells by centrifugation (8000 g, 20 min) the cells were resuspended in resuspension buffer (50 mM Tris/HCl pH 7.4, 100 mM NaCl, 1 mM $MgCl_2$, 10% glycerol, 20 mM Imidazol). Cells were lysed by sonification. A heat treatment step (30 min at 85 °C) followed by centrifugation for 45 min at 15.000 g leads to a pre-purification of the heat stable recombinant MjAgo, which was found in the soluble fraction and was further purified by affinity chromatography using a HisTrap column (GE Healthcare). The protein was eluted in a buffer containing 50 mM Tris/HCl pH 7.4, 100 mM NaCl, 1 mM $MgCl_2$, 10% glycerol, 250 mM imidazol.

For the production of the catalytic mutant $MjAgo^{E541A}$, the MjAgo gene was mutated to introduce an Alanine codon at position E541 using the QuikChange II site-directed mutagenesis kit (Agilent). The recombinant protein was produced in *E. coli* Rosetta(DE3)pLysS cells and extraction of the mutated MjAgo protein was performed as described for the wild-type protein with the exception that the heat treatment step was carried out at 75°C for 30 min. All other mutants were generated using the QuikChange II site-directed mutagenesis kit (Agilent), expressed in *E. coli* Rosetta(DE3)pLysS (50 ml expression cultures) as described for the MjAgo wildtype including a heat treatment step for 30 min at 85°C. MjAgo mutants were purified using Ni-NTA spin columns (Qiagen) according to manufacturer's instructions. Proteins were eluted in the same elution buffer as described for large scale purification via the HisTrap column.

Cloning and preparation of histone A3 from Methanocaldococcus jannaschii

The gene encoding M. jannaschii histone A3 was cloned from genomic DNA using PCR. Following PCR amplification, cloning into pGEM-T (Promega) and sequence verification, the A3 insert was subcloned into the expression vector pET21a(+) (Novagen) using NdeI and XhoI restriction sites. The resulting pET-A3 vector was

transformed into the Rosetta2 expression strain (Novagen), grown in rich media supplemented with ampicillin (100 µg/ml) and induced with 1 mM IPTG for 3 hours. The expression culture was harvested by centrifugation and soluble proteins extracted in N100 extraction buffer (100 mM NaCl, 25 mM Tris-acetate pH 8.0, 10 mM MgCl2, 1 mM DTT) supplemented with EDTA-free protease inhibitor cocktail (Roche) by using a cell press in the presence of 20 µl DNaseI (2500 U/ml) and 20 µl RNase (10 mg/ml). The extract was centrifuged for 30 minutes at 15000 g at 4˚C to remove cell debris. The cleared lysate was heat treated at 70˚C for 30 minutes followed by centrifugation at 13,000 g for 30 minutes at 4˚C to remove denatured E. coli proteins. The supernatant was loaded onto a 1 ml heparin column (HiTrap Heparin HP, GE Healthcare) equilibrated with N100. The protein was eluted with a linear gradient from 0-1.0 M NaCl over 10 CV using N1000 buffer (N100-like buffer containing 1,000 mM NaCl). Fractions containing A3 were pooled and dialyzed (Slide-A-Lyzer Dialysis Cassettes, Life technologies) into N250 buffer (N100-like containing 250 mM NaCl).

Synthetic oligonucleotides and DNAs

DNA guide and target sequences of the let-7 based 20/21mer substrate are listed in Figure 1A. The sequences of the 41 nt long DNA substrate is as follows:

41 nt guide: 5'- ACGGACATTACGAGGTAGTAGGTTGTATAGTCTTATCACCT

41 nt target: 5'-AGGTGATAAGACTATACAACCTACTACCTCGTAATGTCCGT.

All oligonucleotides were HPLC-purified and purchased from MWG (Ebersberg, Germany).

Plasmid DNA used for MjAgo activity assays throughout this work were either standard pGEX-2TK or pET21(a) based vectors. Plasmid DNA was purified from *E. coli* DH5α cells using the HiSpeed Plasmid Midi Kit (Qiagen).

Genomic DNA from *M. jannaschii* was prepared using the DNeasy Blood and Tissue Kit (Qiagen) followed by RNase digestion (Thermo Scientific) of remaining tRNA and rRNA. Genomic DNA from *P. furiosus* was kindly provided by Winfried Hausner (Institute for Microbiology and Archaea Centre, University Regensburg). Genomic DNA from *S. acidocaldarius* was prepared using the Genelute^{TM} Bacterial genome DNA kit (Sigma).

Purification of chromatin from M. jannaschii biomass

1 g *M. jannaschii* biomass (~7*109 cells/g) was resuspended in 20 ml PBS (including protease inhibitor cocktail, Roche) and centrifuged at low speed at 1,500 g for 10 minutes at 4˚C to remove black residue from the culture medium (mostly FeS). The supernatant was transferred to a new tube and, if necessary, the wash step repeated 2-3 x until the pellet has a white appearance. The supernatant was centrifuged at high speed at 14,000 g for 10 minutes at 4˚C in order to pellet the cells. After removal of the supernatant, the cell pellet was carefully resuspended by pipetting in 5 ml chromatin extraction buffer (25 mM HEPES pH 7, 15 mM $MgCl_2$, 100 mM NaCl, 400 mM sorbitol and 0.5 % Triton X-100). The chromatin extract was incubated for 30 minutes at 4˚C and aliquoted into 100 µl portions. Following centrifugation at 14,000 g for 15 minutes at 4 ˚C, the supernatant was removed and the chromatin pellet resuspended in 50 µl extraction buffer, snapfrozen in liquid Nitrogen and stored at -80˚ C.

Activity assays

DNA-guided cleavage assays were performed by combining 3 µM recombinant MjAgo with 0.33 µM guide DNA and 0.67 µM target DNA in a buffer containing 50 mM Tris/HCl pH 7.4, 100 mM NaCl, 5 mM $MgCl_2$, 2% glycerol, 10 mM DTT, and 67 µg/ml BSA in a total volume of 15 µl. The target DNA and the resulting cleavage products are detected via the fluorescent signal of the coupled fluorophore (see Figures for coupling sites). All components were combined at room temperature and the enzymatic reaction was initiated by incubating the samples at 85 °C. 10 µl of the reactions were stopped by the addition of 10 µl formamide-loading buffer and the resulting fragments were separated on a 12% denaturing polyacrylamide gel for 80 min at 70W. The fluorescent signal was visualised using a FLA7000 scanner (GE Healthcare).

Cleavage assays using a dsDNA PCR fragment, circular plasmid DNA (pGEX-2TK vector) or genomic DNA was performed in a buffer containing 50 mM Tris/HCl pH 7.4, 100 mM NaCl, 5 mM $MgCl_2$, 2% glycerol, 10 mM DTT, and 67 µg/ml BSA in a total volume of 10 µl. If not noted otherwise reactions contained 1 µM MjAgo. DNA

concentrations are given in the figure legends. Samples were incubated at 37°C, 75°C or 85°C (see figure legends). Reactions including the catalytic mutant were incubated at 75°C due to the reduced heat stability of the mutated protein. Reactions were stopped at the given time points (see figure legends) by the addition of 1 volume 6M urea and incubation for 5 min at 85°C.

1 µl of Green Buffer (Thermo Fisher, Fast Digest Kit) was added prior to analysis of the sample using agarose gel electrophoresis. For guide-dependent plasmid cleavage reactions a pET21(a) plasmid was used and two matching standard guide sequences were designed that target each strand of the T7 promoter sequence encoded in the pET21 plasmid (T7 fw guide: 5'-PHO-CCCTATAGTGAGTCGTATTA, T7 rev guide: 5'-PHO-CTCACAATTCCCCCATAGTG). Samples were incubated for 5 min at 85°C prior to separation and analysis via agarose gel electrophoresis (1xTAE running buffer including 1 M urea in the buffer and gel).

For MjAgo-mediated cleavage assays that included the histone A3, 14.3 µM histone A3 was pre-incubated with 1.5 µg dsDNA (PCR fragment, 750 bp) in 50 mM Tris/HCl pH 7.4, 100 mM NaCl, 5 mM $MgCl_2$, 2% glycerol, 10 mM DTT, and 67 µg/ml BSA for 10 min at 65°C. Subsequently, 1 µM MjAgo was added and the sample incubated at 85°C (see figure legends for incubation times). Reaction were stopped by fast cooling to 4°C followed by purification of the DNA using the PCR purification kit from Qiagen. Samples were incubated for 5 min at 85°C prior to separation and analysis via agarose gel electrophoresis (1xTAE running buffer).

Isolation and radiolabelling of DNA degradation products after MjAgo-mediated plasmid digestion

Plasmid DNA digest was conducted as described above. One part of the degraded DNA was 5'-dephosphorylated using Antarctic phosphatase (NEB) and purified via Sephadex-G50 columns (GE Healthcare) to remove excess phosphate. Subsequently, dephosphorylated as well as untreated samples of the plasmid DNA fragments were radioactively labelled with [γ-^{32}P] ATP (Perkin Elmer) using T4 PNK (Thermo Fisher Scientific). Modified DNA fragments were purified from excess [γ-^{32}P] ATP using Sephadex G50 columns (GE Healthcare). Labelling success was controlled using liquid scintillation counting. A radioactively labelled size marker was created by digesting

RNA (5'-GCC UCA GCA CGU AAC UCU ATT-3') carrying a radioactive 5'-phosphate using RNase T1 (Thermo Fisher Scientific). Samples were adjusted to equal counts according to liquid scintillation counting, mixed with 1 volume loading buffer (95% formamide, 0.025 % (w/v) SDS, 0.025 % bromophenolblue, 0.025 % xylene cyanol, 0.5 mM EDTA) and analysed using 20 % denaturing PAGE followed by autoradiography.

Heterologous expression of MjAgo in Sulfolobus acidocaldarius

S. acidocaldarius MW001 [31] was grown aerobically at 75°C in basal Brock medium[32], supplemented with 0.1% NZ amine, 0.2% dextrin and 20 µg/ml uracil and adjusted to pH 3.5 with sulfuric acid. For solid media the medium was supplemented with 6 mM $CaCl_2$ and 20 mM $MgCl_2$ and 1.2% gelrite. Plates were incubated for 6 days at 75°C.

To express MjAgo in *S. acidocaldarius*, expression plasmids were constructed by cloning the gene encoding MjAgo (*MJ_1321*) into shuttle vector pSVA1551 (Wagner and Albers, unpublished). The latter is a modified derivate of pCmalLacS [33]. To create a catalytically inactive mutant of MjAgo, pSVA1551-MjAgo was mutated using site-directed mutagenesis, introducing an E541A mutation. The plasmids were transformed into *S. acidocaldarius* MW001 as described previously [34]. Transformants were grown in 50 ml Brock medium [32] supplemented with 0.2% NZ-amine to an OD_{600} of around 0.5. Expression was induced by adding 0.4% maltose and incubating the cells for four more hours at 75°C.

To determine the plasmid-sequences of *MJ_1321* in the expression cultures, a PCR was performed on the lysates using MjAgo specific primers [34]. The PCR product was sequenced using the following primers:

MjAgo fw: 5'-CACCATGGTTTTAAATAAAGTTACATATAAAATAAATGC

MJ_1321_internal_1: 5'- CACTGGTTGATGCTCCAAAC

MJ_1321_internal_2: 5'- TGGGACTTGACACTGGATTG

MJ_1321_internal_3: 5' – TACTCCTCTAATAGTGCTTTATC

MjAgo rev: 5' - TTATATGAAATATAAGAATCCATGC

536 ***TEM analysis of MjAgo-DNA complexes***

537 A purified and concentrated solution of MjAgo or MjAgo-DNA complexes (5 µl) was
538 applied to glow-discharged carbon-coated copper grids, washed 2 to 5 times with
539 double distilled water, shortly blotted onto filter paper after each step and negative-
540 stained with 2 % (w/v) uranyl acetate for 20 s [35]. Afterwards, the grids were blotted
541 on filter paper again and air dried for subsequent transmission electron microscopy
542 (TEM). For this, we used a Zeiss EM 912 in combination with an integrated OMEGA
543 energy filter and operated at 80 kV in the zero-loss mode.

544

545 **Statement about replicates in the experimental work**

546 Listed below is how many times the individual experiment shown in the figures were
547 replicated (distinguishing biological and technical replicates).

548 Figure 1a: six replicates (three biological, three technical); Figure 1d: four replicates
549 (one biological, three technical); Figure 1f: four replicates (one biological, three
550 technical); Figure 2a: six replicates (three biological, three technical); Figure 2b: two
551 biological replicates; Figure 2c: seven replicates (three biological, four technical);
552 Figure 2d: five replicates (two biological, three technical); Figure 2e: three technical
553 replicates; Figure 2f: three technical replicates; Figure 3a: five replicates (three
554 biological, two technical); Figure 3b: two three technical replicates; Figure 3c: six
555 replicates (three biological, three technical); Figure 3d: five replicates (two biological,
556 three technical); Figure 3e: six replicates (four biological, two technical); Figure 4b:
557 six replicates (two biological, four technical).

558

559 **Data availability**

560 All data that support the findings of this study are available from the corresponding
561 author upon request.

562

563 **ACKNOWLEDGMENTS**

564 We would like to acknowledge all members of the Grohmann lab and in particular
565 Kevin Kramm for cloning of the MjAgo catalytic mutant. We would like to thank
566 Gunter Meister for fruitful discussions. Work in the Grohmann RNAP laboratory was

567 funded by the Deutsche Forschungsgemeinschaft (GR 3840/2-1). SVA and MvW
568 acknowledge funding by the European Research Council (starting Grant
569 ARCHAELLUM 311523). S. Schn. acknowledges funding by the Deutsche
570 Forschungsgemeinschaft, the excellence cluster CIPSM and Fonds der Chemischen
571 Industrie.
572
573
574 **AUTHOR CONTRIBUTIONS**
575 Conception of the study: DG; experimental work: AZ, SW, MvW, LE, SSt, SO, AK, SB,
576 DG; data analysis: AZ, SW, MvW, SVA, SSchn, DG, AK, FW; writing of the manuscript:
577 DG. All authors edited the manuscript.
578

FIGURE LEGENDS

Figure 1: Guide-directed target cleavage activity of MjAgo using canonical and non-canonical substrates. (a) Guide and target strand sequences used are derived from the human let-7 miRNA and are shown as DNA duplex, which is efficiently cleaved by MjAgo (the Alexa647 (AF647) modification site in the target strand is highlighted in red) [11]. **(b)** Different guide strand lengths (13-23 nt) were used for cleavage reactions (3 µM MjAgo, 1.7 µM DNA_{guide} and 0.72 µM DNA_{target} at 85°C) and the reactions were stopped after 0, 7.5 and 15 min. Cleavage products were resolved on a 12% denaturing polyacrylamide gel. Efficient target strand cleavage requires a minimal guide length of 15 nt. **(c)** Canonical and non-canonical substrates (composed of long guide and long target strands) were used for MjAgo cleavage reactions (fluorophore coupling site is indicated by a red star). **(d)** MjAgo cleaves all offered DNA substrates even when an overlong guide strand of 41 nt is used (0.6 µM MjAgo, 1.7 µM DNA_{guide} and 0.72 µM DNA_{target} at 85°C, time points: 0,15, 20 min). (**e**) Substrates with a fluorescent marker dye positioned either at the 5' or 3' end of the target of a short or long ds DNA substrate. (**f**) MjAgo mediated cleavage pattern of non-canonical substrates shown in (**e**) reveal a stepwise processing of the DNA from the 5'-end of the target.

Figure 2: MjAgo processes long linear and circular double-stranded DNAs and genomic DNA in the absence of a guide DNA. (a) MjAgo mediated cleavage of linear dsDNA (1.1 µM MjAgo, 1 µg PCR product at 85°C, time points: 15, 30, 60, 120 min). (**b**) Transmission electron microscopy (TEM) image of a MjAgo-linear dsDNA sample. Filled arrowheads show proteins (approximately 15-20 nm in diameter) associated with dsDNA indicates standard arrows point to naked dsDNA. Scale bar: 100 nm. (**c**) Time-course of MjAgo-mediated processing of circular plasmid DNA in the absence of DNA guides at 75°C and 85°C (1 µM MjAgo, 1 µg plasmid DNA; time points for cleavage at 75°: 0, 1, 2, 4, 6h; time points for cleavage at 85°C: 0, 2.5, 10, 30, 60 min). (**d**) Comparison of the wildtype (wt) and a catalytic mutant of MjAgo (E541A) in the plasmid DNA cleavage assay at 37°C and 75°C (1 µM MjAgo, 1.1 µg plasmid DNA, time points: 3 and 6 h; - : untreated plasmid DNA, + EcoRI: EcoRI digested plasmid). (**e**) Agarose gel electrophoresis of *M. jannaschii* chromatin and *M.jannaschii* genomic DNA after incubation with MjAgo (7.5 µM MjAgo, 37.7 ng chromatin or 780 ng genomic DNA at 37°C). Sample containing 0.5% triton is a control reaction as the chromatinised DNA was prepared in a buffer containing 0.5% triton. **(f)** Cleavage reaction using linear dsDNA (750 bp) in the presence and absence of *M. jannaschii* histone A3. 1.5 µg dsDNA fragment was incubated with 1 µM MjAgo at 85°C. Samples were taken after 45 and 90 min of incubation and resolved on a 1% Agarose gel. MjAgo mediated degradation is clearly visible in the absence of histones. If the dsDNA is pre-incubated with 14.3 µM *M. jannaschii* histone A3, the DNA is protected against MjAgo degradation (time points 0, 45, 90 min).

Figure 3: Characterisation of DNA degradation products and influence on MjAgo-mediated plasmid degradation. (a) Final degradation products of a MjAgo-mediated plasmid DNA degradation that has run to completion (1 µM MjAgo, 1 µg plasmid DNA, 85°C, time points: 0, 2.5, 10, 30, 60, 180 min). (**b**) Final degradation products were extracted, radiolabelled and separated on a 20% denaturing sequencing polyacrylamide gel. (**c**) 1µg pGEX-2TK plasmid was digested to completion with MjAgo (2 µM MjAgo, 2h at 85°C). Subsequently, a fresh aliquot of the same plasmid (1 µg pGEX-2TK) or a plasmid with a different sequence (pET21-derived plasmid) was added to start a new round of cleavage reaction (2 µM MjAgo, 1 µg plasmid DNA at 85°C, time points: 0, 5, 10, 20 min). (**d**) Agarose gel electrophoresis analysis of plasmid DNA incubated with MjAgo in the absence of guide DNA strands (- guide DNA), with MjAgo in the presence of two matching 5'-phosphorylated guides that target each strand of the T7 promoter sequence in the pET-vector, respectively (+ matching guide DNA). In addition, MjAgo in the presence of random non-matching guide DNA was used. Reactions contained 1 µM MjAgo, 600 ng pET plasmid DNA and were incubated for 0, 15, 30 and 60 min at 37°C. (**e**) Agarose gel electrophoresis of co-purified nucleic acids extracted from affinity purified MjAgo (purification at 4°C) after heterologous expression in *E.coli*. Nucleic acids were Phenol/Chloroform extracted from the protein and digested with the nucleases given.

Figure 4: Mutational analysis of MjAgo guide-independent plasmid cleavage activity. (**a**) MjAgo crystal structure in complex with a 21 nucleotide guide strand (PDB: 5G5T). The 5'-end of the guide is anchored in the Mid domain binding pocket (highlighted in teal), the 3'-end is bound in the PAZ domain binding pocket (red). Helix 7 is a flexible element (orange) that undergoes conformational changes and is involved in correct positioning of a target strand (see also Supplementary Figure S9). MjAgo structures revealed the position of a putative third nucleic acid binding channel (light blue) located between the PIWI and N-terminal domain. Positions of the MjAgo point mutations used for plasmid cleavage studies are highlighted. Inset shows the apo MjAgo structure (PDB: 5G5S). Due to a rotation of the PAZ domain, residues N170 and D438 are located in close proximity potentially interacting with each other. (**b**) Agarose gel electrophoreses of the final plasmid degradation products of MjAgo wt and MjAgo mutants (1 µM MjAgo, 300 ng plasmid DNA; cleavage for 2h at 85°C). As a control, the plasmid was incubated in the absence of MjAgo (-) or with MjAgo wt in the presence of EDTA (wt + EDTA).

Figure 5: Putative model of guide-dependent and guide-independent DNA silencing by MjAgo. (a) (1) Invading nucleic acids like plasmid DNA or viral DNA are recognised by MjAgo and will be subject to nucleolytic degradation. *M.jannaschii*'s genomic DNA (gDNA) is protected against MjAgo-mediated degradation as *M.jannaschii* encodes histone proteins that keep the gDNA in a chromatinized state. (2) The first round of guide-independent degradation leads to a primed MjAgo with accelerated MjAgo-mediated cleavage of DNA in a second cleavage round. One priming mechanism is the incorporation of short DNA fragments generated during the first wave of DNA degradation. These DNAs can serve as guide to direct guide-dependent

671 silencing of invasive nucleic acids. **(b)** Genomic location of MjAgo (Mj_1321). Blast
672 search in the KEGG genome database revealed that MjAgo is encoded in a cluster
673 with three hypothetical proteins, showing similarities to enzymes involved in rRNA
674 processing (Mj_1320, RNase motif) and DNA recombination /repair (Mj_1322:
675 exonuclease SbcC, Mj_1323: DNA repair protein RAD32).
676
677
678
679
680
681
682
683
684
685
686
687
688
689
690
691
692
693
694
695
696
697
698
699
700
701
702
703

REFERENCES

1. Willkomm, S., Zander, A., Gust, A. & Grohmann, D. A prokaryotic twist on argonaute function. *Life* **5**, 538-53 (2015).
2. Swarts, D.C. et al. The evolutionary journey of Argonaute proteins. *Nature structural & molecular biology* **21**, 743-53 (2014).
3. Meister, G. Argonaute proteins: functional insights and emerging roles. *Nature reviews. Genetics* **14**, 447-59 (2013).
4. Elbashir, S.M. et al. Duplexes of 21-nucleotide RNAs mediate RNA interference in cultured mammalian cells. *Nature* **411**, 494-8 (2001).
5. Elbashir, S.M., Lendeckel, W. & Tuschl, T. RNA interference is mediated by 21- and 22-nucleotide RNAs. *Genes & development* **15**, 188-200 (2001).
6. Zamore, P.D., Tuschl, T., Sharp, P.A. & Bartel, D.P. RNAi: double-stranded RNA directs the ATP-dependent cleavage of mRNA at 21 to 23 nucleotide intervals. *Cell* **101**, 25-33 (2000).
7. Swarts, D.C. et al. Argonaute of the archaeon Pyrococcus furiosus is a DNA-guided nuclease that targets cognate DNA. *Nucleic acids research* **43**, 5120-9 (2015).
8. Swarts, D.C. et al. DNA-guided DNA interference by a prokaryotic Argonaute. *Nature* **507**, 258-61 (2014).
9. Wang, Y. et al. Structure of an argonaute silencing complex with a seed-containing guide DNA and target RNA duplex. *Nature* **456**, 921-6 (2008).
10. Wang, Y. et al. Nucleation, propagation and cleavage of target RNAs in Ago silencing complexes. *Nature* **461**, 754-61 (2009).
11. Zander, A., Holzmeister, P., Klose, D., Tinnefeld, P. & Grohmann, D. Single-molecule FRET supports the two-state model of Argonaute action. *RNA biology* **11**, 45-56 (2014).
12. Gao, F., Shen, X.Z., Jiang, F., Wu, Y. & Han, C. DNA-guided genome editing using the Natronobacterium gregoryi Argonaute. *Nature biotechnology* (2016).
13. Willkomm, S., Zander, A., Grohmann, D. & Restle, T. Mechanistic Insights into Archaeal and Human Argonaute Substrate Binding and Cleavage Properties. *PloS one* **11**, e0164695 (2016).
14. Ma, J.B. et al. Structural basis for 5'-end-specific recognition of guide RNA by the A. fulgidus Piwi protein. *Nature* **434**, 666-70 (2005).
15. Schirle, N.T. & MacRae, I.J. The crystal structure of human Argonaute2. *Science* **336**, 1037-40 (2012).
16. Wang, Y., Sheng, G., Juranek, S., Tuschl, T. & Patel, D.J. Structure of the guide-strand-containing argonaute silencing complex. *Nature* **456**, 209-13 (2008).
17. Frank, F., Sonenberg, N. & Nagar, B. Structural basis for 5'-nucleotide base-specific recognition of guide RNA by human AGO2. *Nature* **465**, 818-22 (2010).
18. Nakanishi, K., Weinberg, D.E., Bartel, D.P. & Patel, D.J. Structure of yeast Argonaute with guide RNA. *Nature* **486**, 368-74 (2012).
19. Kaya, E. et al. A bacterial Argonaute with noncanonical guide RNA specificity. *Proceedings of the National Academy of Sciences of the United States of America* (2016).

20. Olovnikov, I., Chan, K., Sachidanandam, R., Newman, D.K. & Aravin, A.A. Bacterial argonaute samples the transcriptome to identify foreign DNA. *Molecular cell* **51**, 594-605 (2013).
21. Miyoshi, T., Ito, K., Murakami, R. & Uchiumi, T. Structural basis for the recognition of guide RNA and target DNA heteroduplex by Argonaute. *Nature communications* **7**, 11846 (2016).
22. Blow, M.J. et al. The Epigenomic Landscape of Prokaryotes. *PLoS genetics* **12**, e1005854 (2016).
23. Loenen, W.A., Dryden, D.T., Raleigh, E.A., Wilson, G.G. & Murray, N.E. Highlights of the DNA cutters: a short history of the restriction enzymes. *Nucleic acids research* **42**, 3-19 (2014).
24. Willkomm, S., Oellig, C.A., Zander, A., Restle, T., Keegan, R., Grohmann, D., Schneider, S. Structural and mechanistic insights into an archaeal DNA-guided Argonaute protein. . *under consideration for back-to-back publication in Nature Microbiology* (2016).
25. Elkayam, E. et al. The structure of human argonaute-2 in complex with miR-20a. *Cell* **150**, 100-10 (2012).
26. Peeters, E., Driessen, R.P., Werner, F. & Dame, R.T. The interplay between nucleoid organization and transcription in archaeal genomes. *Nature reviews. Microbiology* **13**, 333-41 (2015).
27. Cheloufi, S., Dos Santos, C.O., Chong, M.M. & Hannon, G.J. A dicer-independent miRNA biogenesis pathway that requires Ago catalysis. *Nature* **465**, 584-9 (2010).
28. Chandradoss, S.D., Schirle, N.T., Szczepaniak, M., MacRae, I.J. & Joo, C. A Dynamic Search Process Underlies MicroRNA Targeting. *Cell* **162**, 96-107 (2015).
29. Schirle, N.T., Sheu-Gruttadauria, J. & MacRae, I.J. Gene regulation. Structural basis for microRNA targeting. *Science* **346**, 608-13 (2014).
30. Parker, J.S. How to slice: snapshots of Argonaute in action. *Silence* **1**, 3 (2010).
31. Wagner, M. et al. Expanding and understanding the genetic toolbox of the hyperthermophilic genus Sulfolobus. *Biochemical Society transactions* **37**, 97-101 (2009).
32. Brock, T.D., Brock, K.M., Belly, R.T. & Weiss, R.L. Sulfolobus: a new genus of sulfur-oxidizing bacteria living at low pH and high temperature. *Archiv fur Mikrobiologie* **84**, 54-68 (1972).
33. Berkner, S., Wlodkowski, A., Albers, S.V. & Lipps, G. Inducible and constitutive promoters for genetic systems in Sulfolobus acidocaldarius. *Extremophiles : life under extreme conditions* **14**, 249-59 (2010).
34. Wagner, M. et al. Versatile Genetic Tool Box for the Crenarchaeote Sulfolobus acidocaldarius. *Frontiers in microbiology* **3**, 214 (2012).
35. Rachel, R. et al. Analysis of the ultrastructure of archaea by electron microscopy. *Methods in cell biology* **96**, 47-69 (2010).

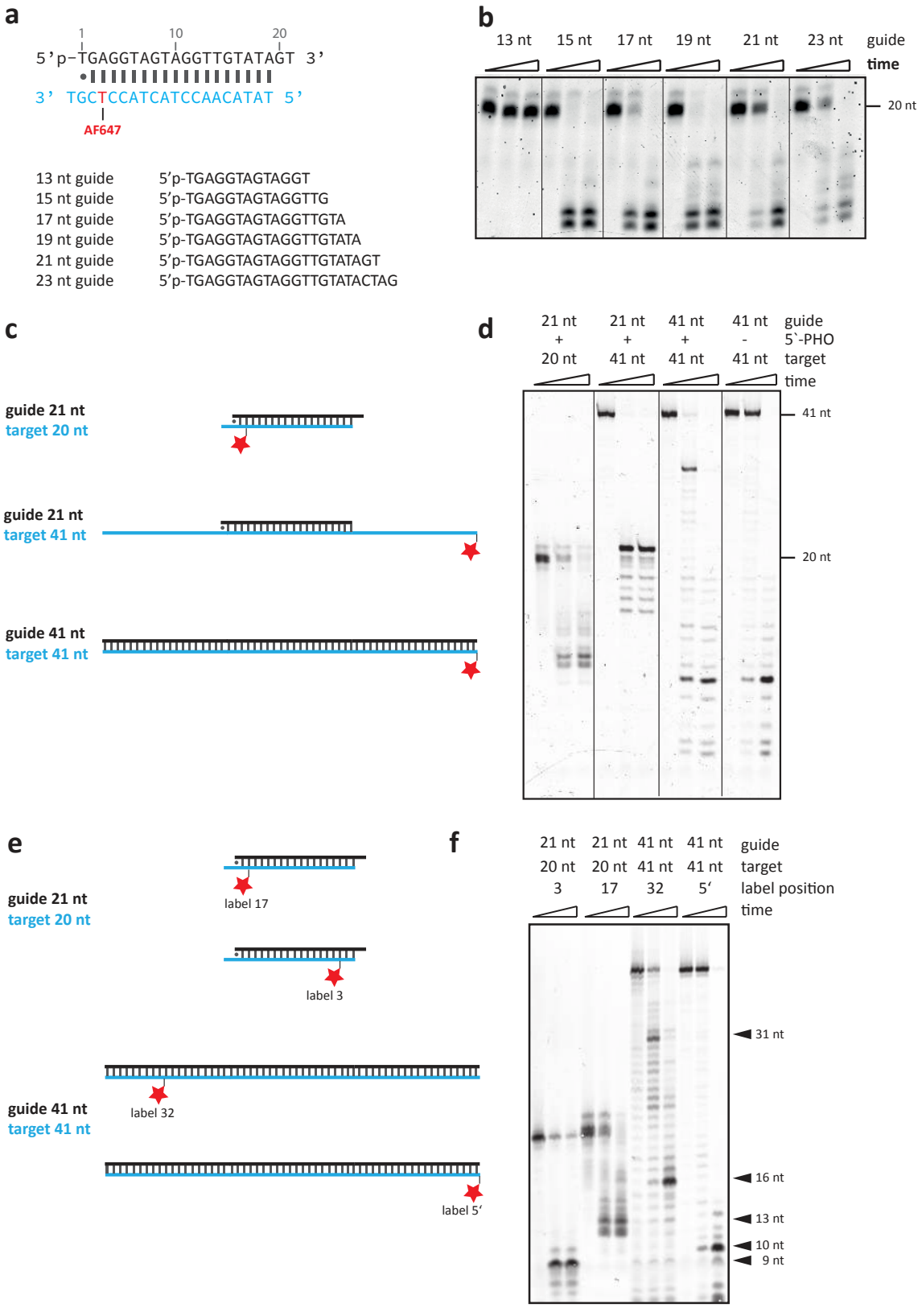
a
1
10
20
5'p-TGAGGTAGTAGGTTGTATAGT 3'
3' TGCTCCATCATCCAACATAT 5'
AF647
13 nt guide 5'p-TGAGGTAGTAGGT
15 nt guide 5'p-TGAGGTAGTAGGTTG
17 nt guide 5'p-TGAGGTAGTAGGTTGTA
19 nt guide 5'p-TGAGGTAGTAGGTTGTATA
21 nt guide 5'p-TGAGGTAGTAGGTTGTATAGT
23 nt guide 5'p-TGAGGTAGTAGGTTGTATACTAG
b
13 nt
15 nt
17 nt
19 nt
21 nt
23 nt
guide
time
20 nt
c
guide 21 nt
target 20 nt
guide 21 nt
target 41 nt
guide 41 nt
target 41 nt
d
21 nt + 20 nt
21 nt + 41 nt
41 nt + 41 nt
41 nt - 41 nt
guide
5`-PHO
target
time
41 nt
20 nt
e
guide 21 nt
target 20 nt
label 17
label 3
guide 41 nt
target 41 nt
label 32
label 5'
f
21 nt 20 nt 3
21 nt 20 nt 17
41 nt 41 nt 32
41 nt 41 nt 5'
guide
target
label position
time
31 nt
16 nt
13 nt
10 nt
9 nt

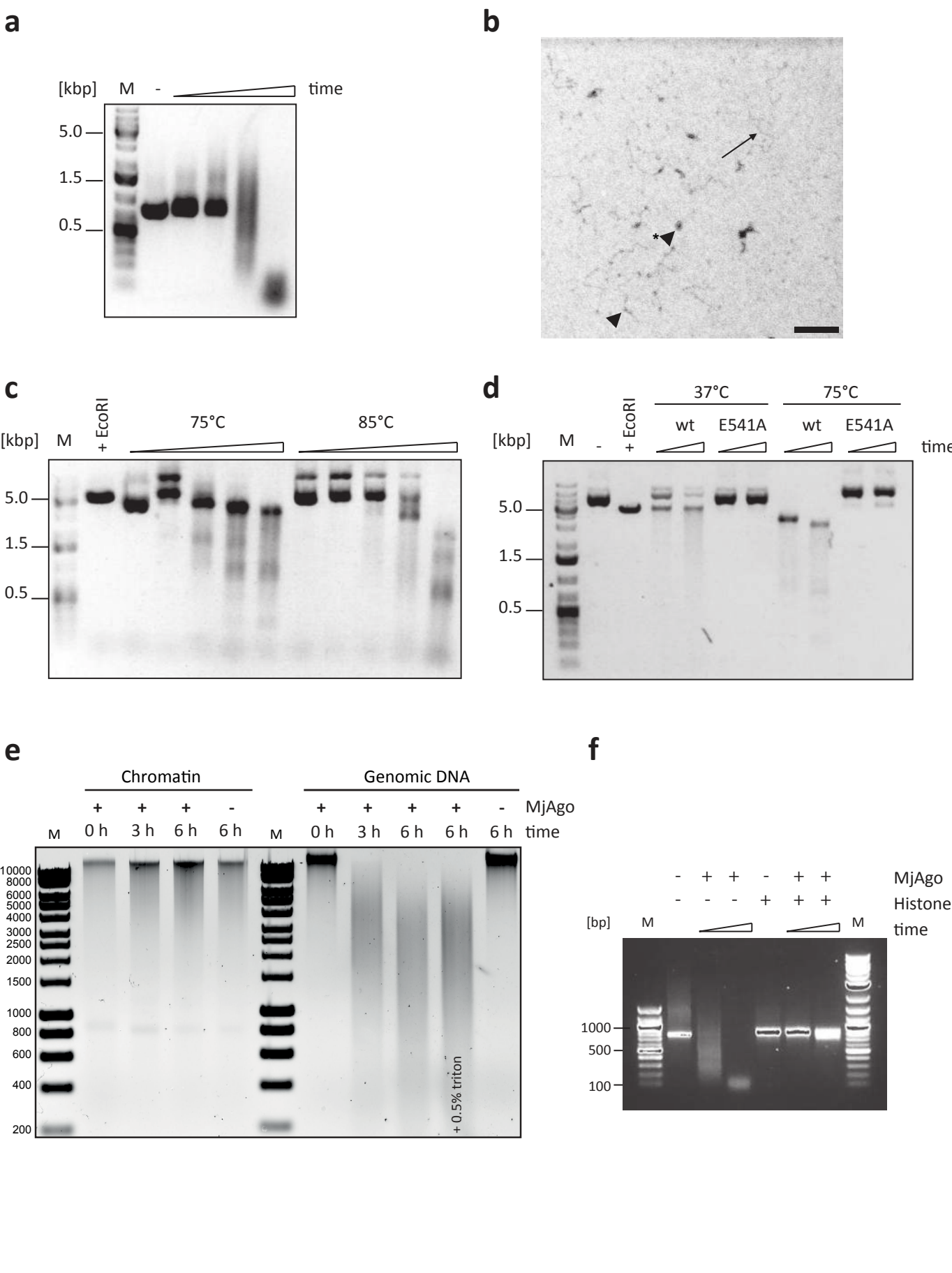
a
[kbp]
M
-
time
5.0
1.5
0.5
b
*
c
[kbp]
M
+ EcoRI
75°C
85°C
5.0
1.5
0.5
d
[kbp]
M
-
+ EcoRI
37°C
75°C
wt
E541A
wt
E541A
time
5.0
1.5
0.5
e
Chromatin
Genomic DNA
+
+
+
-
+
+
+
+
-
MjAgo
M
0 h
3 h
6 h
6 h
M
0 h
3 h
6 h
6 h
6 h
time
10000
8000
6000
5000
4000
3000
2500
2000
1500
1000
800
600
400
200
+ 0.5% triton
f
-
+
+
-
+
+
MjAgo
-
-
-
+
+
+
Histone
[bp]
M
time
M
1000
500
100

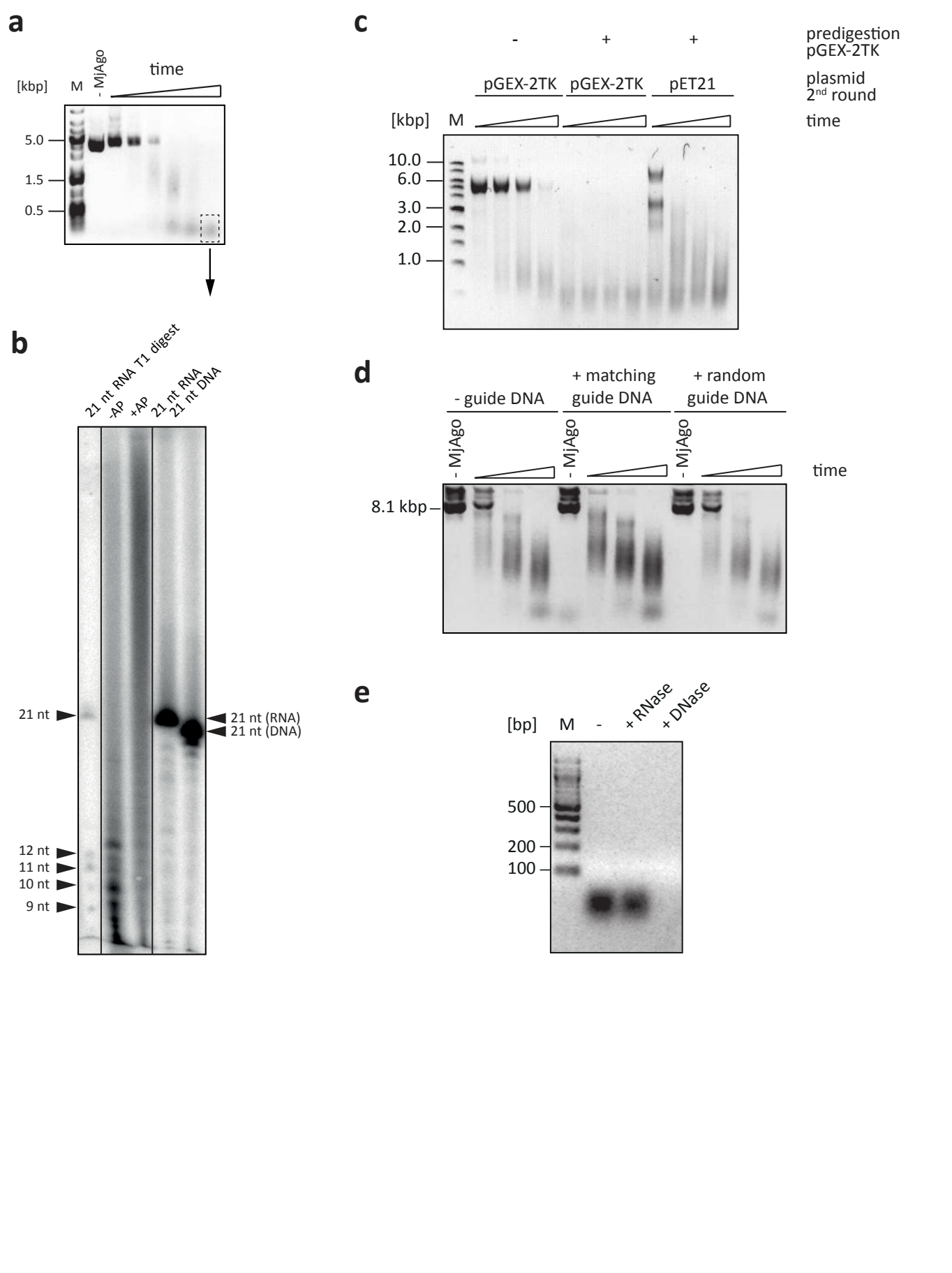
a
[kbp]
M
- MjAgo
time
5.0
1.5
0.5
b
21 nt RNA T1 digest
-AP
+AP
21 nt RNA
21 nt DNA
21 nt
12 nt
11 nt
10 nt
9 nt
21 nt (RNA)
21 nt (DNA)
c
-
+
+
predigestion
pGEX-2TK
pGEX-2TK
pGEX-2TK
pET21
plasmid
2nd round
[kbp]
M
time
10.0
6.0
3.0
2.0
1.0
d
- guide DNA
+ matching
guide DNA
+ random
guide DNA
- MjAgo
- MjAgo
- MjAgo
time
8.1 kbp
e
[bp]
M
-
+ RNase
+ DNase
500
200
100

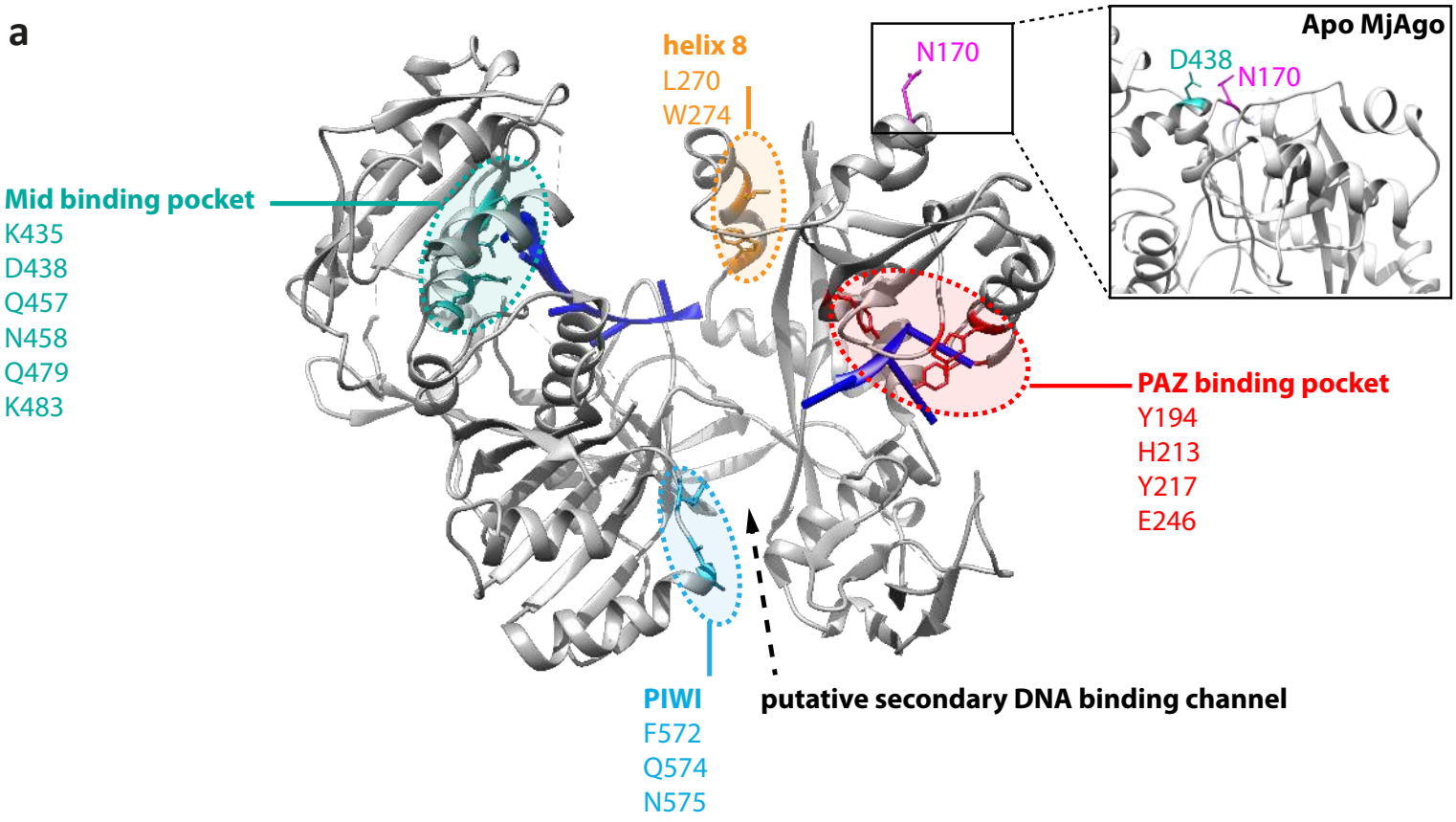
a
helix 8
L270
W274
N170
Apo MjAgo
D438
N170
Mid binding pocket
K435
D438
Q457
N458
Q479
K483
PAZ binding pocket
Y194
H213
Y217
E246
PIWI
F572
Q574
N575
putative secondary DNA binding channel

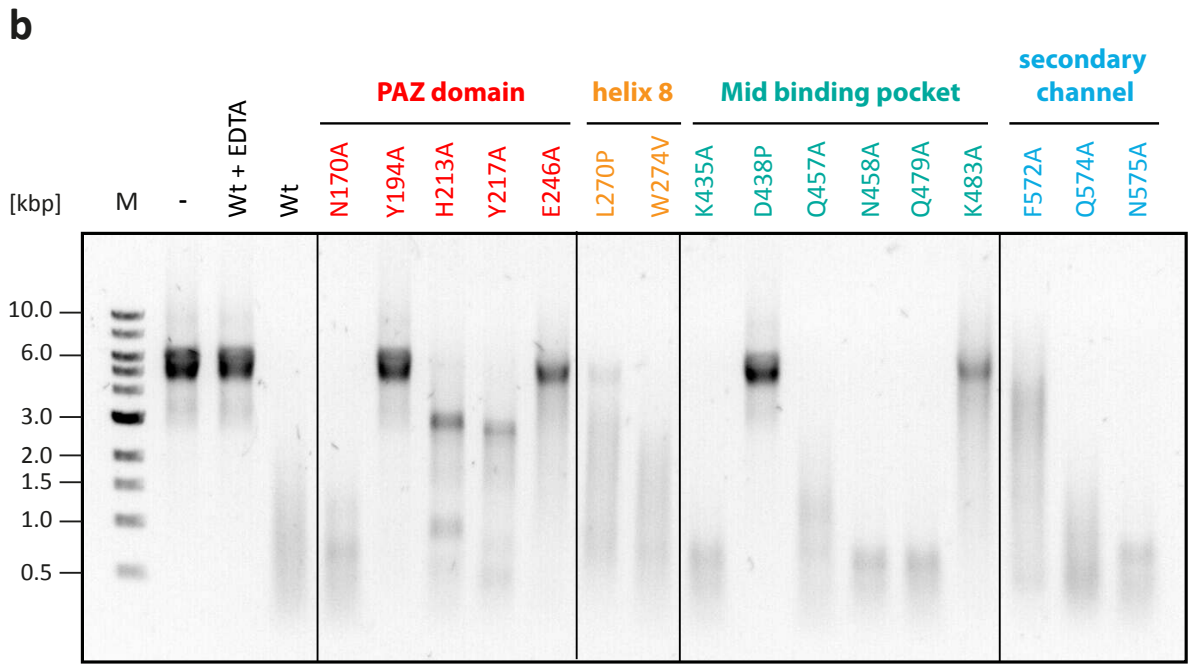
b
PAZ domain
helix 8
Mid binding pocket
secondary channel
[kbp]
M
-
Wt + EDTA
Wt
N170A
Y194A
H213A
Y217A
E246A
L270P
W274V
K435A
D438P
Q457A
N458A
Q479A
K483A
F572A
Q574A
N575A
10.0
6.0
3.0
2.0
1.5
1.0
0.5

a

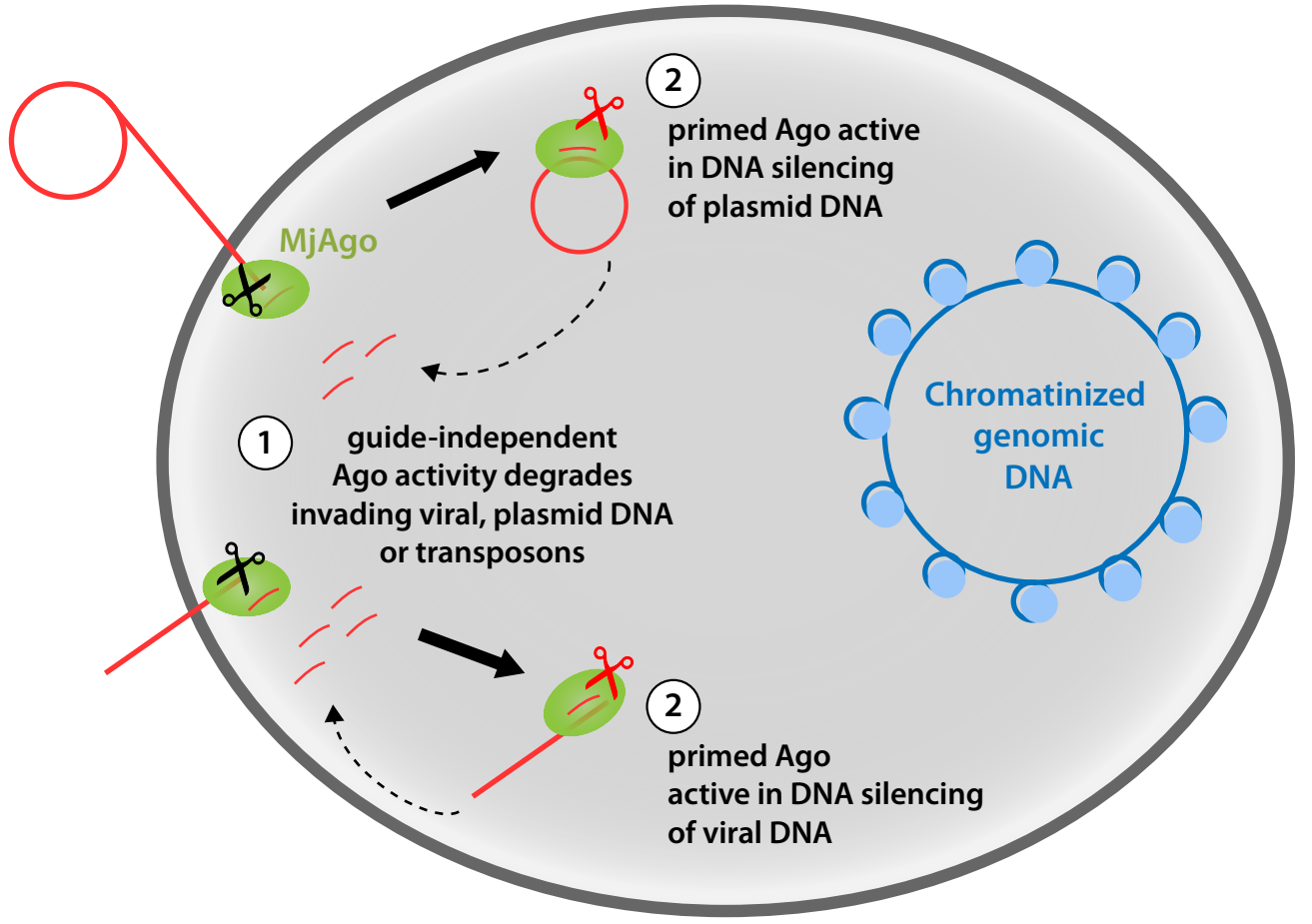

guide-independent unspecific nucleolytic activity of MjAgo

guide-dependent nucleolytic activity of a primed MjAgo

Supplementary Information

Guide-independent DNA cleavage by archaeal Argonaute from *Methanocaldococcus jannaschii*

Adrian Zander[1], Sarah Willkomm[1], Sapir Ofer[2], Marleen van Wolferen[3], Luisa Egert[1], Sabine Buchmeier[4], Sarah Stöckl[1], Philip Tinnefeld[4], Sabine Schneider[5], Andreas Klingl[6], Sonja-Verena Albers[3], Finn Werner[2], Dina Grohmann[1]

Supplementary Methods

Generation of MjAgo monoclonal antibodies

Mouse monoclonal antibodies against recombinant MjAgo were raised at the Antibody Facility Braunschweig (Germany). Monoclonal antibodies were generated by immunizing mice with recombinant MjAgo protein according to a standard immunization protocol. After hybridization and cloning, antibody producing hybridoma cells were screened by ELISA for their ability to bind recombinant MjAgo protein. The specificity of the antibody was checked by immunoblot. Isotype analysis of the 7D9 clone against MjAgo revealed an IgG1 subtype. Antibody-containing supernatants were gained according to standard protocols. The experimental protocols were carried out in accordance with the Directive 2010/63/EU of the European Parliament and the Council of the European Union of 22 September 2010 and all procedures were approved by guidelines from the Animal Committee on Ethics in the Care and Use of Laboratory Animals of TU Braunschweig, Germany (Az §5 (02.05) TschB TU BS).

Western Blotting and Immunodetection

M. jannaschii cell mass was obtained from the Archaeen Zentrum (University Regensburg). For immunodetection of MjAgo in *M. jannaschii* cell extracts, proteins in the cell extract were resolved by 15% SDS-PAGE, transferred to nitrocellulose membranes (Bio-Rad) using a semi-dry blotting system (Bio-Rad), and immunodetection was performed using TBS-T buffer with 5% caseine as blocking reagent. The blots were incubated with the mouse antisera and Alexa647-conjugated goat anti-mouse IgG (Life Technologies) as secondary antibody, scanned on a FLA-5000 scanner (GE Lifesciences) equipped with a 635 nm excitation laser. For immunodetection of MjAgo expressed in *S. acidocaldarius*, whole cell fractions were loaded on an 11% SDS-PAGE gel and analysed by Western-blotting. MjAgo was detected using the anti-MjAgo antibody as primary antibody and HRP conjugated anti-mouse antibodies (Pierce) as secondary antibody. The protein was visualised using Clarity Western ECL Blotting Substrate (Bio-Rad).

Isolation and enzymatic digestion of co-purified nucleic acids

In order to detect and isolate nucleic acids that co-purify with MjAgo upon recombinant expression of MjAgo in *E. coli*, cell lysis and MjAgo preparation via Ni-NTA affinity

chromatography was carried out at 4°C, which keeps the nucleic acid-MjAgo complexes intact. After elution of MjAgo from the Ni-NTA columns, co-purified nucleic acids were isolated by phenol-chloroform extraction followed by Ethanol precipitation. Isolated nucleic acids were treated with either RNase (Thermo Fisher) or DNaseI (Thermo Fisher) according to manufacturer's instructions. The nucleic acids were analysed via Agarose gel electrophoresis.

Supplementary Figures

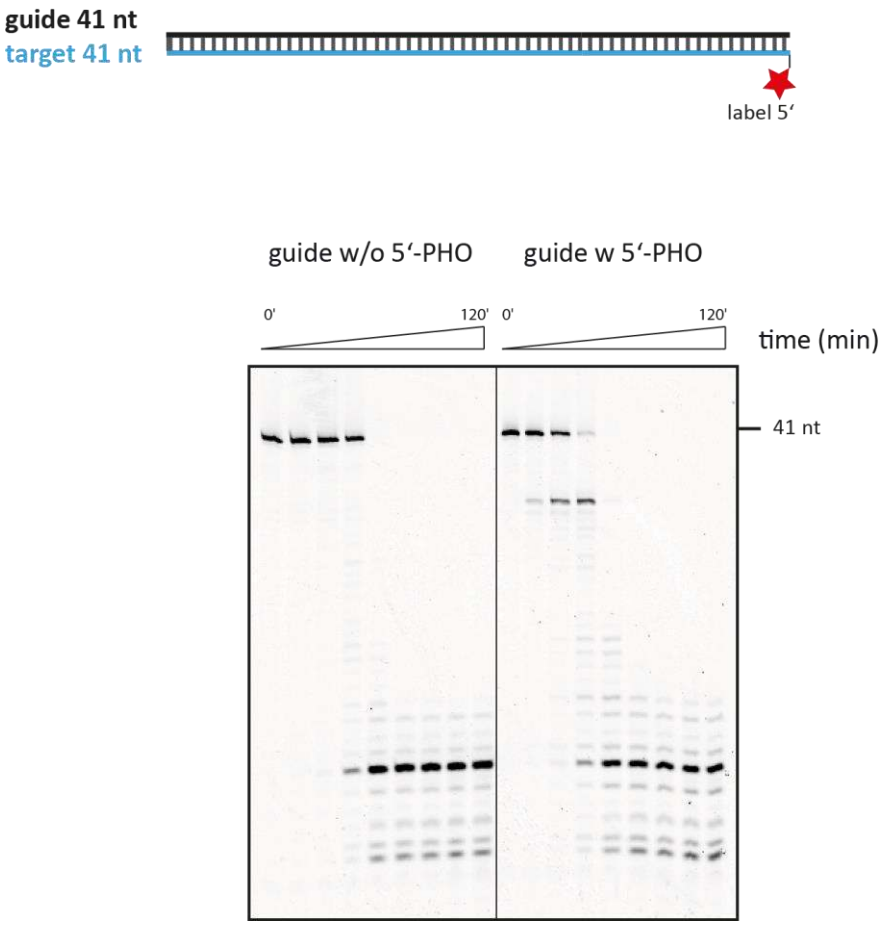

Supplementary Figure 1: MjAgo mediated cleavage of non-canonical substrates. A 41 nt long guide with and without phosphate group at the 5’-end of the guide strand (5’-PHO) was used for a cleavage reaction. Substrates were incubated with 3 µM MjAgo wt, 0.33 µM DNA_{guide} and 0.67 µM DNA_{target} at 85°C and reactions were stopped after 0, 5, 10, 15, 20, 30, 60, 90 and 120 min. Cleavage products were resolved on a 15% denaturing polyacrylamide gel. A 5’-phosphate group at the guide directs a fast cleavage reaction with association of 5’-end the guide in the Mid-binding MjAgo leading to a cleavage product at the canonical cleavage site opposite bases 9-10 of the guide. This reaction competes with a slower cleavage reaction. Here, MjAgo starts degradation of the DNA from the 5’-end of the target. Three independent experiments (technical replicates) were carried out and a representative gel is shown.

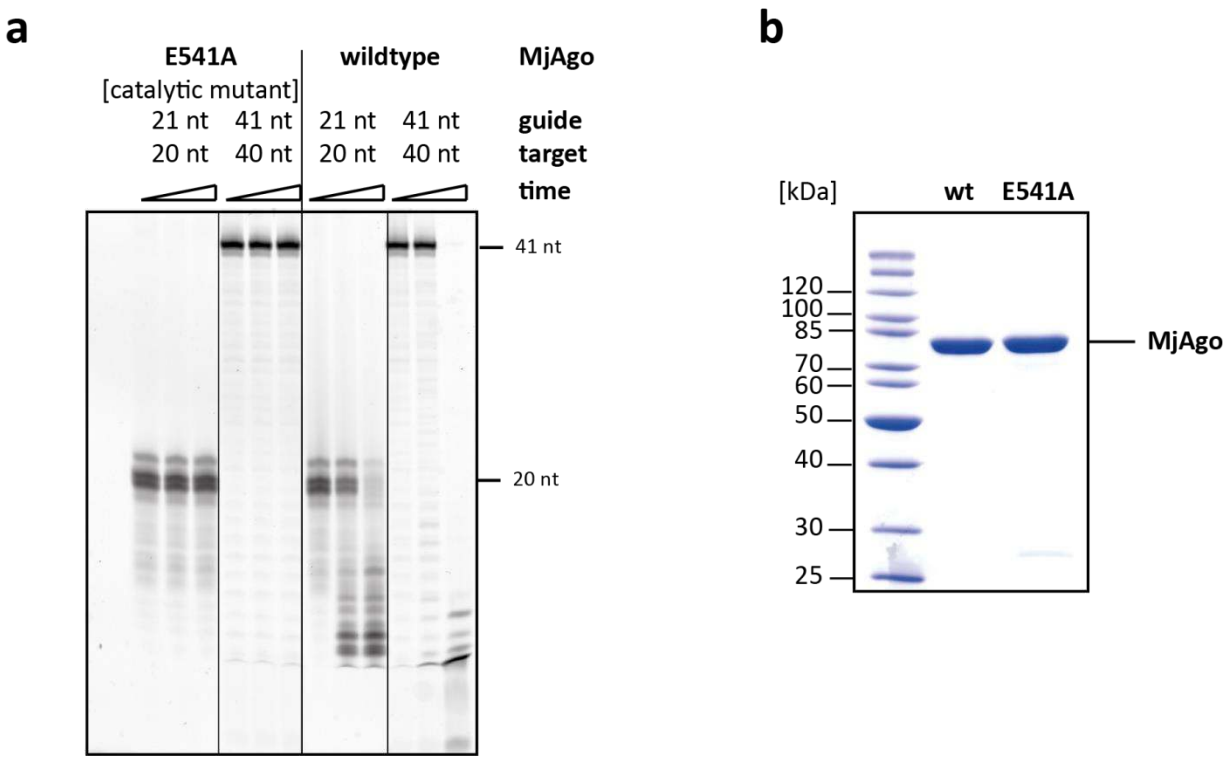

Supplementary Figure 2: Guide-directed target cleavage activity of MjAgo and the catalytic mutant MjAgo^{E541A} using canonical and non-canonical substrates. (a) The guide and target strand sequences are derived from the human let-7 miRNA (see Figure 1 for sequences). Substrates were incubated with 3 µM MjAgo or MjAgo^{E541A}, 0.33 µM DNA_{guide} and 0.67 µM DNA_{target} at 85°C and reactions were stopped after 0, 7.5 and 15 min. Cleavage products were resolved on a 15% denaturing polyacrylamide gel. No cleavage of the substrate was observed when the catalytic mutant was used. Four independent experiments (one biological and three technical replicates) were carried out and a representative gel is shown. **(b)** SDS-PAGE (10%) analysis of purified MjAgo wt and the catalytic mutant MjAgo^{E541A}. MjAgo was purified via a 6x histidine tag. The gel was stained with Coomassie Brilliant Blue. The position of MjAgo (theoretical molecular weight: 84.5 kDa) is indicated. Three independent experiments (technical replicates) were carried out and a representative gel is shown.

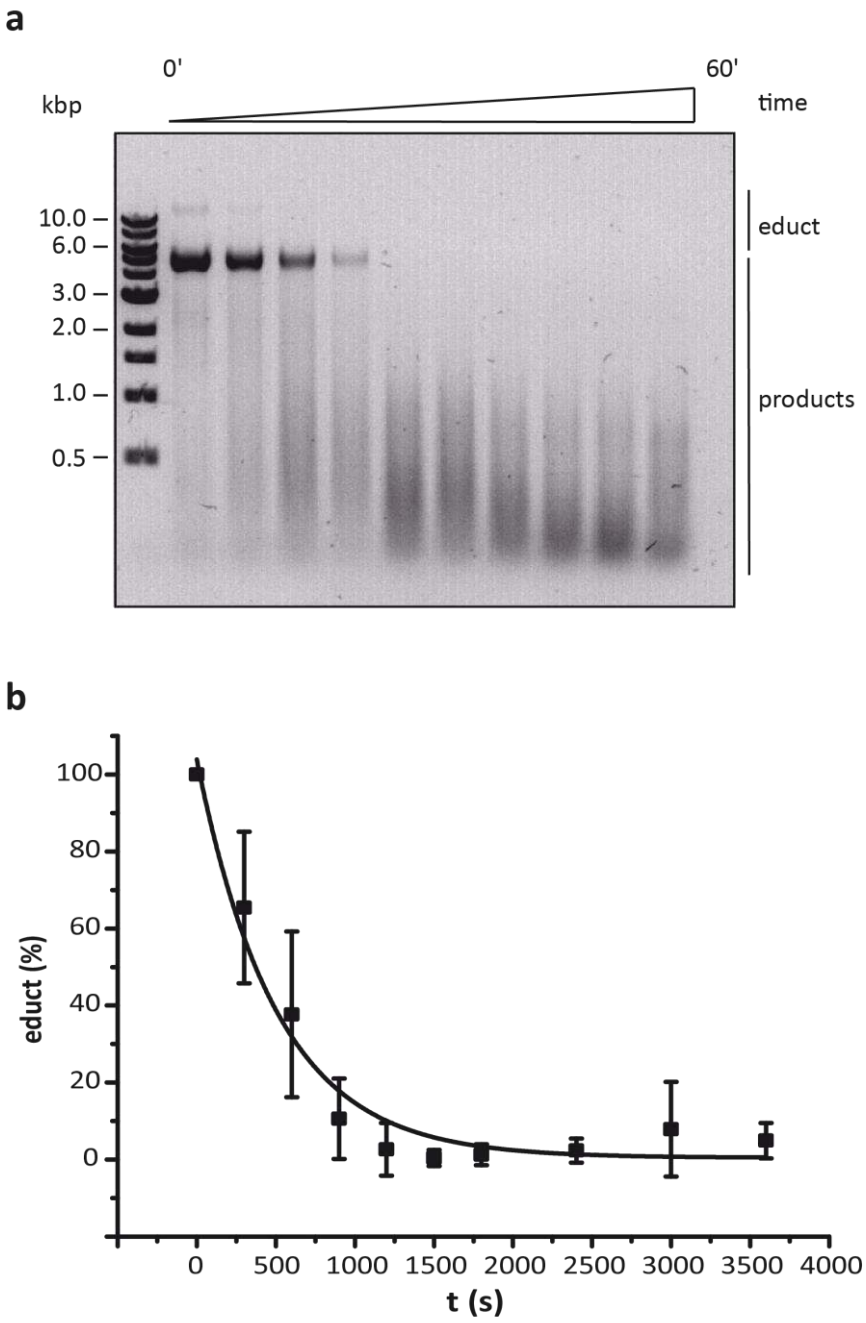

Supplementary Figure 3: Time-resolved MjAgo-mediated plasmid cleavage. (a) Plasmid cleavage reactions (2 µM MjAgo and 400 ng Plasmid per 10 µL reaction) were carried out at 85°C. Samples were taken after 0', 5', 10', 15', 20', 25', 30', 40', 50' and 60'. Samples were separated on 0.5% agarose gels. Three independent experiments (technical replicates) were carried out and a representative gel is shown. **(b)** The intensities of the educt bands were quantified (average of three independent experiments with error bars representing the standard deviations are plotted against the time) and the intensity at time point 0' has been set to 100%. The other band intensities were normalized accordingly. The decrease of educt intensity was mathematically analyzed using a single exponential equation yielding a rate constant of 0.002 ± 0.0003 s^{-1}.

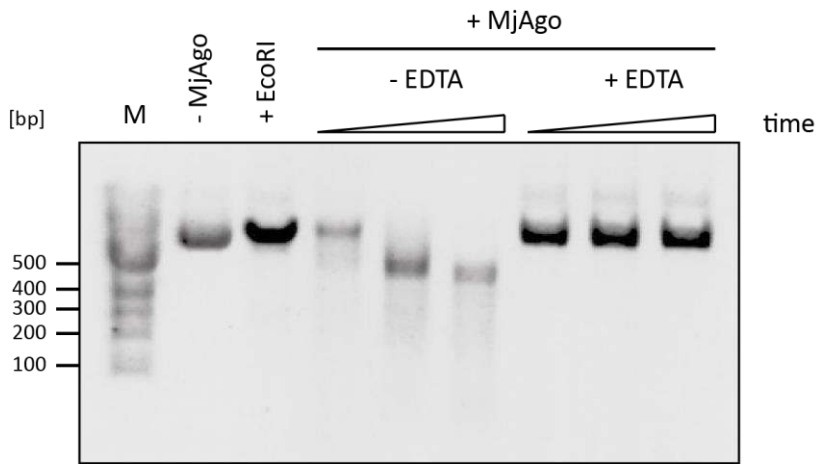

Supplementary Figure 4: MjAgo mediated plasmid cleavage requires divalent cations. MjAgo-mediated cleavage of circular plasmid DNA in the absence of DNA guides at 85°C in the presence and absence of EDTA (1.1 µM MjAgo, 1.6 µg plasmid DNA; time points: 15, 30, 60 min. + EcoRI: EcoRI digested plasmid). Six independent experiments (two biological and four technical replicates) were carried out and a representative gel is shown.

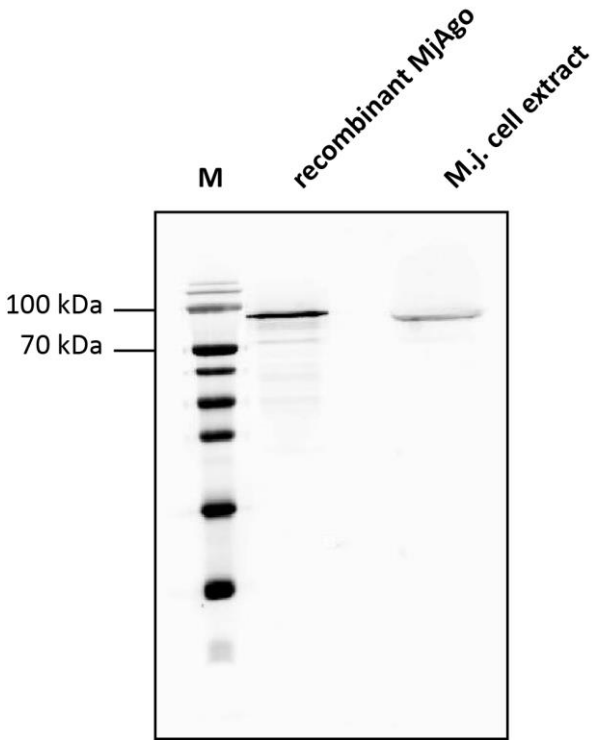

Supplementary Figure 5: Endogenous MjAgo level. Immunoblot analysis to detect endogenous MjAgo in *M. jannaschii* cell extract. Recombinant MjAgo (254 ng) is loaded for comparison (left). Three independent experiments (technical replicates) were carried out and a representative gel is shown.

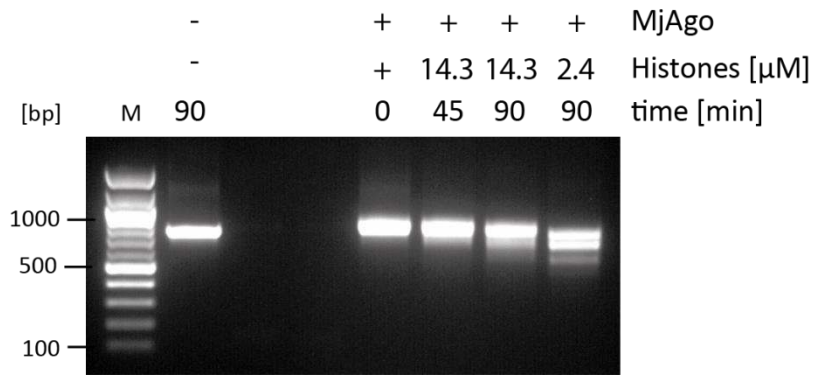

Supplementary Figure 6: **Histone A3 protects DNA against MjAgo-mediated cleavage.** MjAgo cleavage reaction of dsDNA (750 bp) in the presence and absence of *M. jannaschii* histone A3. 1.5 µg dsDNA fragment was incubated with 1 µM MjAgo at 85°C. If the dsDNA is pre-incubated with 14.3 µM *M. jannaschii* histone A3, the DNA is protected against MjAgo degradation (time points 0, 45, 90 min). If reduced concentrations of histone A3 are used (2.4 µM), a regular ladder-like pattern emerges suggesting that MjAgo has access to regularly spaced unprotected DNA sites. Samples were resolved on a 1% Agarose gel. Three independent experiments (technical replicates) were carried out and a representative gel is shown.

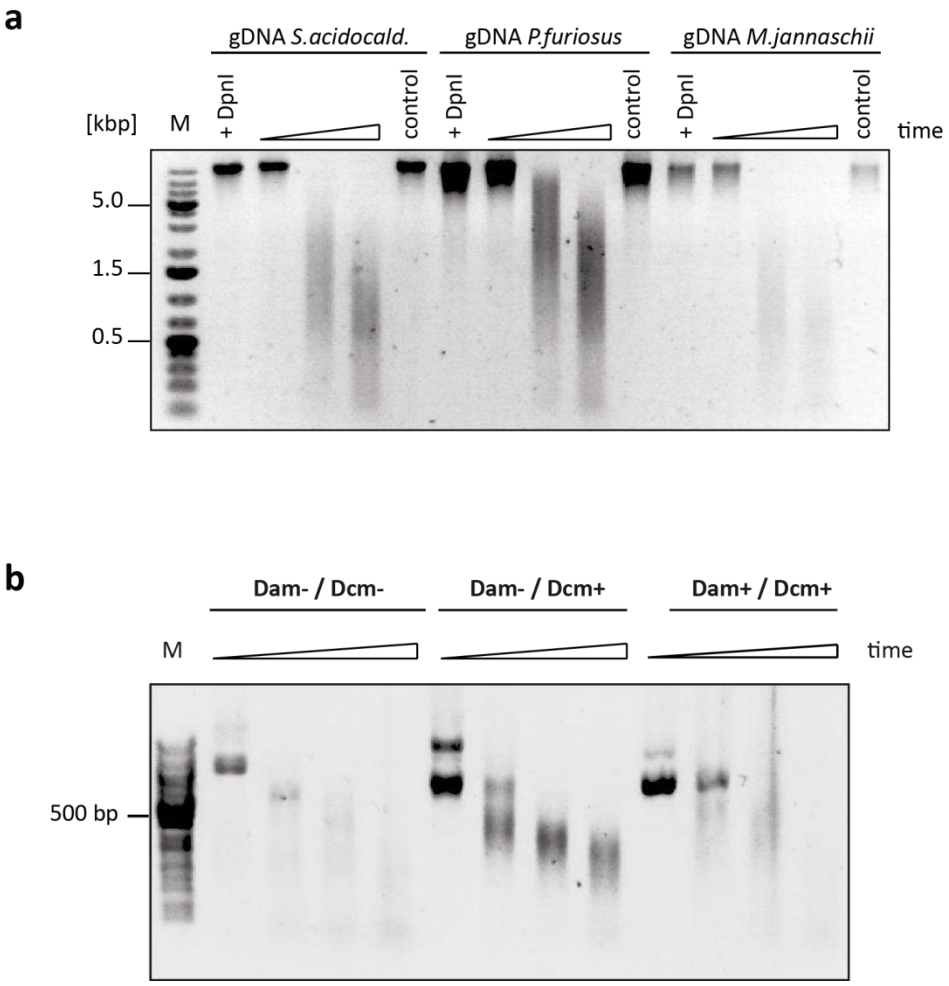

Supplementary Figure 7: **MjAgo degrades genomic DNA from different archaeal organisms and plasmid with different methylation pattern.** (**a**) Agarose gel electrophoresis analysis of gDNA from the archaeal organisms *Sulfolobus acidocaldarius*, *Pyrococcus furiosus* and *Methanocaldococcus jannaschii* after incubation with MjAgo (1 µM MjAgo, 1 µg genomic DNA, reactions were carried out at 37°C, time points: 0, 3 and 6h). Control reaction: incubation of the respective genomic DNA for 6h at 37°C in the absence of MjAgo. Six independent experiments (three biological and three technical replicates) were carried out and a representative gel is shown. (b) Agarose gel electrophoresis analysis of plasmid DNA with different methylation pattern. After incubation with MjAgo (1.1 µM MjAgo, 400 ng plasmid DNA, reactions were carried out at 85°C, time points: 0, 15, 30 and 60 min). Five independent experiments (two biological and three technical replicates) were carried out and a representative gel is shown. Dam- and Dcm-: plasmids were propagated in *E. coli* strains that lack either the Dam methylase (Dam-) or Dcm methylase (Dcm-) or both (Dam-/Dcm-). Dam- plasmids are not methylated at the N6 position of adenine in the sequence GATC. Dcm- plasmids are not methylated at the C5 position of the second cytosine in the sequence CCAGG and CCTGG.

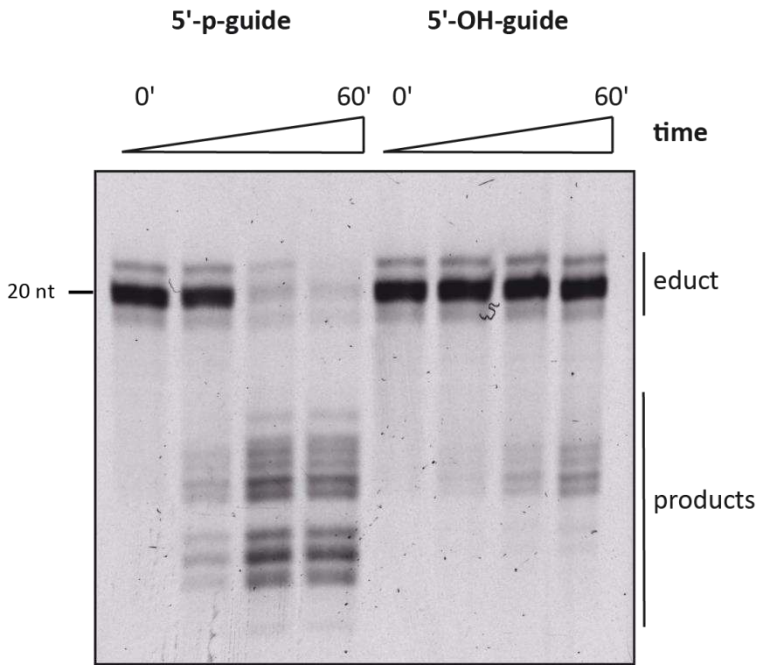

Supplementary Figure 8: MjAgo-dependent target cleavage mediated by either 5'-phosphorylated or 5'-hydroxylated guide strands. 1 µM MjAgo, 340 nM DNA_{guide} and 680 nM DNA_{target} were incubated at 85°C. Samples were taken at time points 0', 15', 30' and 60' and separated using 15% denaturing PAGE. Three independent experiments (technical replicates) were carried out and a representative gel is shown.

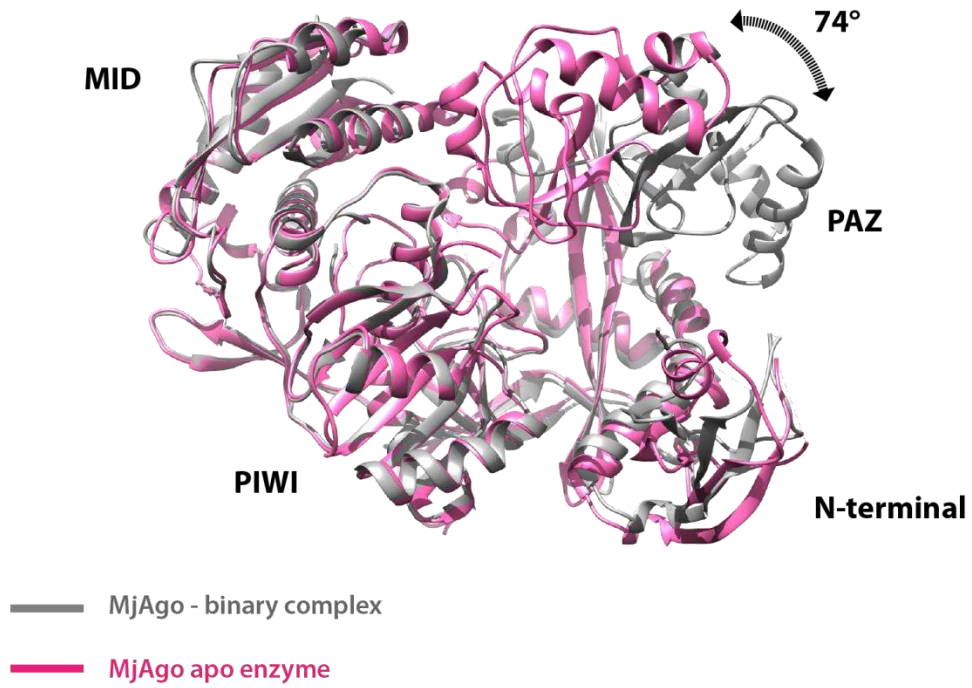

Supplementary Figure 9: Structural comparison MjAgo apo enzyme and MjAgo in complex with a guide DNA (binary complex). Structural alignment of MjAgo in its unliganded apo form (PDB: 5G5S) and MjAgo in complex with a 21nt canonical guide DNA (PDB: 5G5T, DNA not shown). Loading of a DNA guide results in a significant conformational change of the PAZ domain of MjAgo, e.g. the rotation of the PAZ domain by 74° opens up the bilobal enzyme.

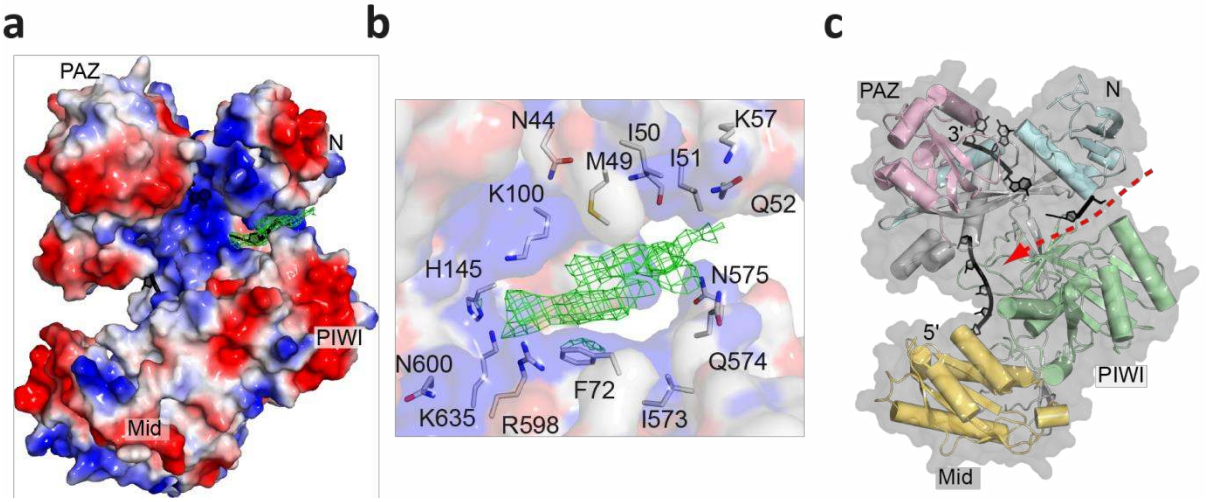

Supplementary Figure 10: Putative secondary nucleic acid-binding channel in the X-ray crystal structure of the MjAgo binary complex. (a) Surface representation of MjAgo, coloured according to amino acid charges (blue=positive, red=negative). In the cleft between PIWI and N-domain positive simulated-annealing omit difference electron density, (contoured at 2.5 Å, green), can be observed, which hints at the presence of nucleobases. **(b)** A semi-transparent protein surface representation is overlaid over the ribbon of the MjAgo binary complex. The potential secondary nucleic acid binding cleft is indicated by the red arrow. **(c)** Zoom in the cleft between N- and PIWI domain, with surrounding residues shown as stick model (PDB code 5G5T).

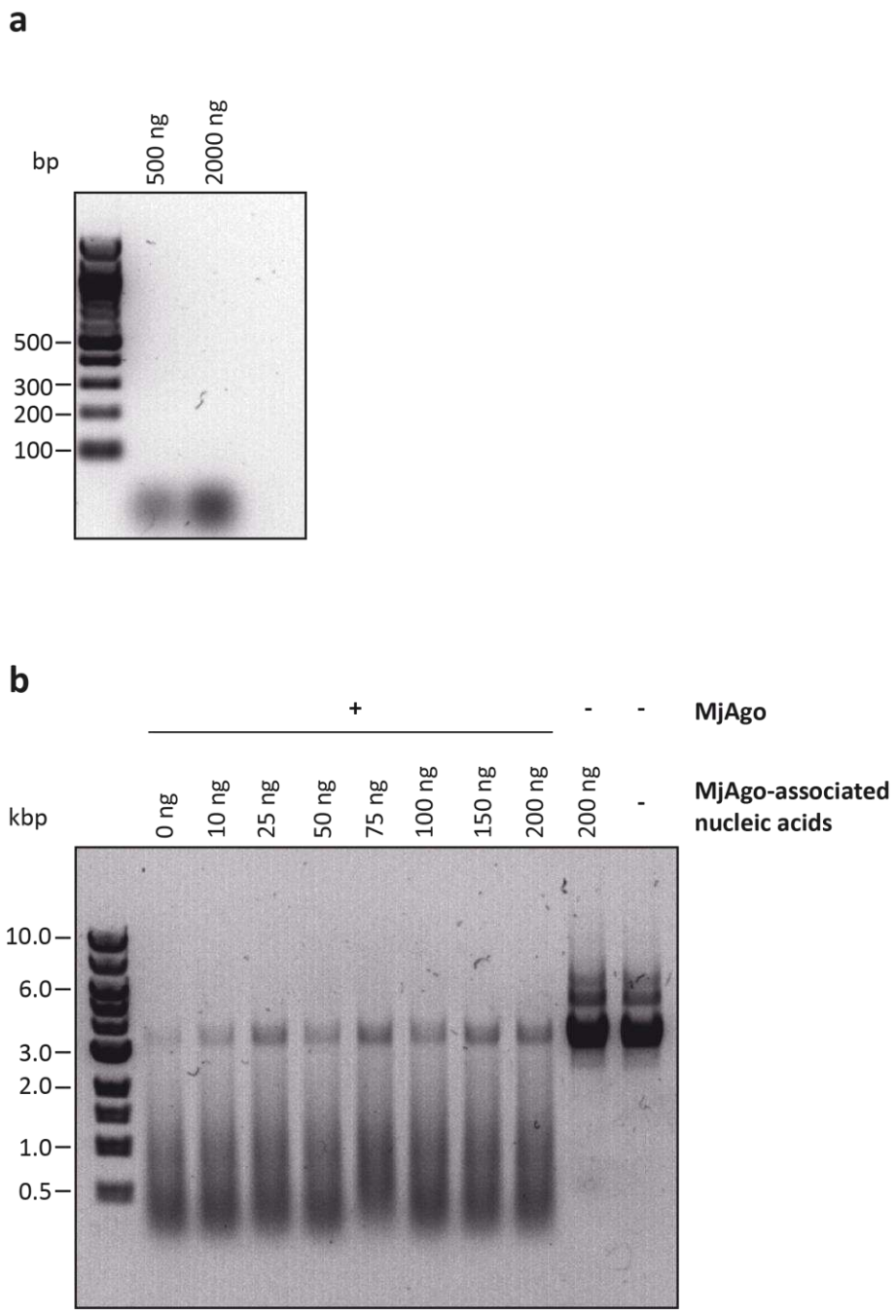

Supplementary Figure 11: MjAgo plasmid cleavage activity in presence of co-purified DNAs. (a) MjAgo-associated nucleic acids were isolated after MjAgo preparation at 4°C using phenol-chloroform extraction followed by ethanol precipitation of the nucleic acids. Defined amounts (500 and 2000 ng) were separated on a 1.5 % agarose gel. Three independent experiments (biological replicates) were carried out and a representative gel is shown. **(b)** Plasmid cleavage assays (3 µM MjAgo and 400 ng plasmid per 10 µL reaction at 85°C for 10 min) have been conducted in presence of increasing concentrations of nucleic acids that co-purify with MjAgo. Reaction products were separated using 0.5 % agarose gel supplemented with 1 M urea. Three independent experiments (technical replicates) were carried out and a representative gel is shown.

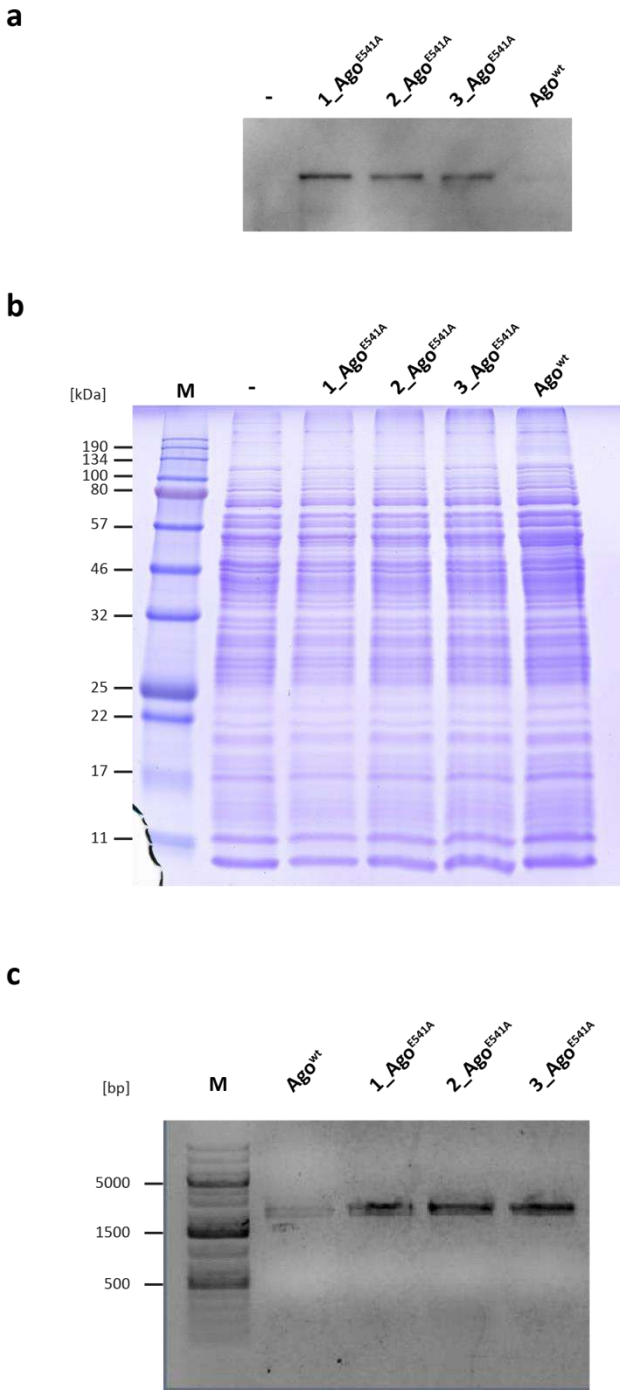

Supplementary Figure 12: Hetereologeous expression of MjAgo in S. acidocaldarius. (**a**) Immunoblot analysis to detect MjAgo heterologously expressed in *S. acidocaldarius*. Wildtype MjAgo is expressed at significant lower levels compared to the catalytic mutant E541A. (**b**) SDS-polyacrylamid separation of *S. acidocaldarius* cell extracts expressing MjAgo wt or the catalytic mutant E541A shows that total protein amount used for the immunodetection in panel A is comparable. (**c**) PCR amplification of MjAgo gene from the samples used in (A) shows that the reduced MjAgo protein level is due to a reduced concentration of MjAgo expression plasmid maintained in *S. acidocaldarius* cells when transformed with the MjAgo wt expression plasmid. Two independent experiments (biological replicates) were carried out and representative gels are shown.

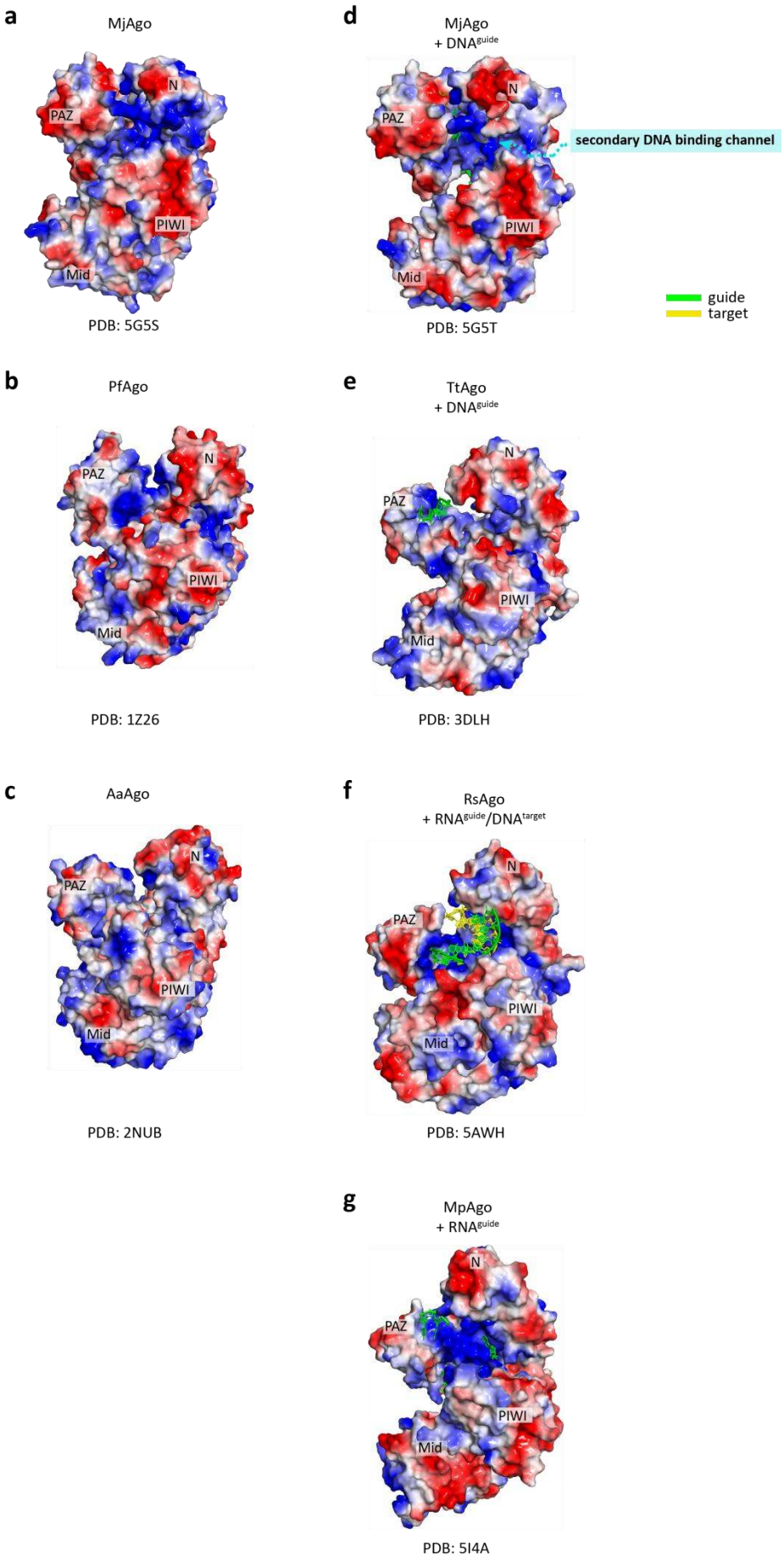

Supplementary Figure 13. Amino acid charges (blue=positive, blue = negative) are mapped on the surface of prokaryotic Argonaute structures. (**d**) Electron density was found in the cleft between PIWI and N-domain of MjAgo hinting at the presence of nucleobases. This cleft is lined by positively charged amino acids suggesting a putative secondary nucleic acid binding channel. A comparable channel is not present in any other prokaryotic Ago.